

# UHV Techniques

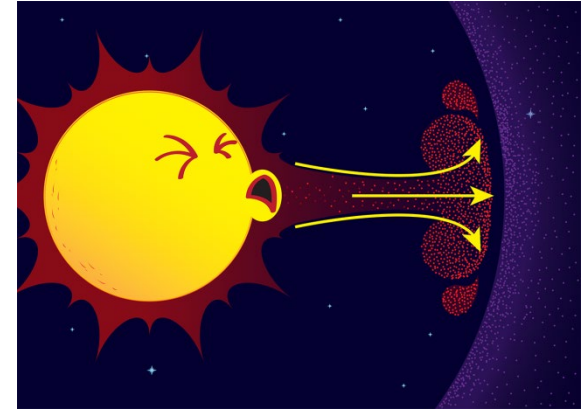
As part of the course 'Molecular Aspects of Catalysts and Surfaces'  
529-0611-00L

Dr. Luca Artiglia  
Paul Scherrer Institut  
luca.artiglia@psi.ch

# What is Vacuum?

The term VACUUM can be used to describe these conditions:

1) Complete absence of matter (definite volume in which gases are almost absent – e.g. interstellar space)



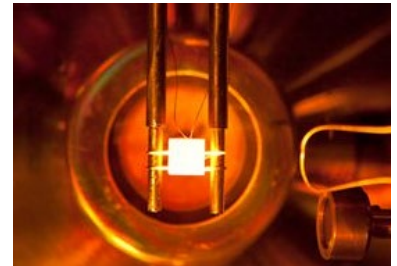
2) Physical state in which the pressure in a definite volume is smaller than in the surroundings (e.g. smaller than the atmospheric pressure)



An example:  $\rho_{\text{gas}} = 2 \cdot 10^{19} \text{ mol/cm}^3$  (atmospheric pressure)  
 $\rho_{\text{gas}} = 10^9 \text{ mol/cm}^3$  (orbiting satellite)

# Some applications of Vacuum

- Reduce the concentration of a gas below a critical level (e.g.  $O_2$  in bulbs)
- Avoid gas-driven physico-chemical processes (e.g. experiments studying the gas-surface interaction) and increase the mean free path of particles (e.g. ion and electron spectroscopies)
- Thermal insulation
- Degasification of liquids



## Vacuum classification

Vacuum	Pressure (torr)	Number Density ( $\text{m}^{-3}$ )	M.F.P. (m)	Surface Collision Freq. ( $\text{m}^{-2}\cdot\text{s}^{-1}$ )	Monolayer Formation Time (s)
Atmosphere	<b>760</b>	$2.7 \times 10^{25}$	$7 \times 10^{-8}$	$3 \times 10^{27}$	$3.3 \times 10^{-9}$
Rough	$10^{-1}$ - <b><math>10^{-3}</math></b>	$3.5 \times 10^{19}$	0.05	$4 \times 10^{21}$	$2.5 \times 10^{-3}$
High	$10^{-3}$ - <b><math>10^{-6}</math></b>	$3.5 \times 10^{16}$	50	$4 \times 10^{18}$	2.5
Very high	$10^{-6}$ - <b><math>10^{-9}</math></b>	$3.5 \times 10^{13}$	$50 \times 10^3$	$4 \times 10^{15}$	$2.5 \times 10^3$
Ultrahigh	$10^{-9}$ - <b><math>10^{-12}</math></b>	$3.5 \times 10^{10}$	$50 \times 10^6$	$4 \times 10^{12}$	$2.5 \times 10^6$ (29 days!)

# Gas flow regimes

**The mean free path** is the average distance that a gas molecule can travel before colliding with another molecule and is determined by:

- Size of molecule (2r)
- Pressure (p)
- Temperature (T)

$$\lambda_a = \frac{k}{\pi\sqrt{2}} \cdot \frac{T}{(2r)^2 p}$$

Vacuum range	Pressure in hPa (mbar)	Pressure in mmHg (Torr)	Molecules / cm <sup>3</sup>	Molecules / m <sup>3</sup>	Mean free path
Ambient pressure	1013	759.8	$2.7 \times 10^{19}$	$2.7 \times 10^{25}$	68 nm <sup>[2]</sup>
Low vacuum	300 – 1	225 – $7.501 \times 10^{-1}$	$10^{19} - 10^{16}$	$10^{25} - 10^{22}$	0.1 – 100 $\mu$ m
Medium vacuum	$1 - 10^{-3}$	$7.501 \times 10^{-1} - 7.501 \times 10^{-4}$	$10^{16} - 10^{13}$	$10^{22} - 10^{19}$	0.1 – 100 mm
High vacuum	$10^{-3} - 10^{-7}$	$7.501 \times 10^{-4} - 7.501 \times 10^{-8}$	$10^{13} - 10^9$	$10^{19} - 10^{15}$	10 cm – 1 km
Ultra-high vacuum	$10^{-7} - 10^{-12}$	$7.501 \times 10^{-8} - 7.501 \times 10^{-13}$	$10^9 - 10^4$	$10^{15} - 10^{10}$	1 km – $10^5$ km
Extremely high vacuum	$<10^{-12}$	$<7.501 \times 10^{-13}$	$<10^4$	$<10^{10}$	$>10^5$ km

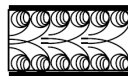
The gas in a vacuum system can be in a **viscous state**, in a **molecular state** (or in a transition state) depending on the dimensionless parameter know as the **Knudsen number** ( $K_n$ ) that is the ratio between the mean free path and the characteristic dimension of the flow channel.

$$K_n = \frac{\lambda_a}{a}$$

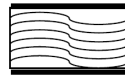
$\lambda_a$  = mean free path  
 $a$  = characteristic dimension of flow channel  
 (typically a pipe radius)

Viscous Flow :

$$Kn = \frac{\lambda_a}{a} < 0.01$$



Turbulent



Laminar

Transition Flow :

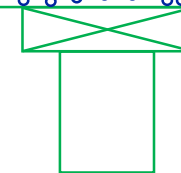
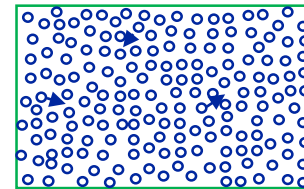
$$0.01 < Kn < 1.0$$

Molecular Flow :

$$Kn > 1.0$$

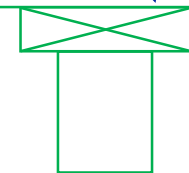
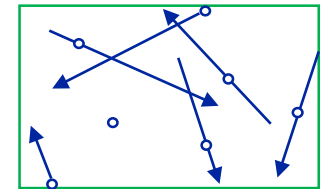


Molecular



**Viscous Flow**  
 (momentum transfer  
 between molecules)

**$P > 1$  mbar**



**Molecular Flow**  
 (molecules move  
 independently)

**$P < 10^{-3}$  mbar**

# Creation of Vacuum: pumping technology

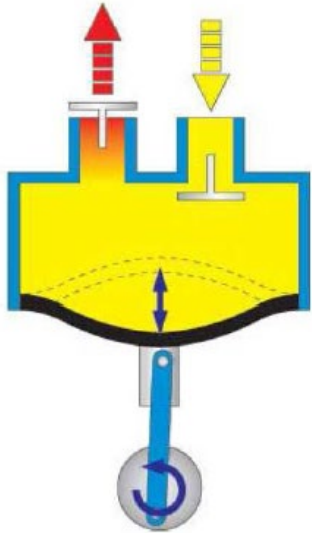
1) **Primary pumping systems:** mechanical pumps that decrease the pressure from atmospheric pressure pressures close to the ultra-high vacuum ( $10^{-6}$ - $10^{-8}$  mbar)

- Rough pumps (atmospheric pressure down to  $10^{-3}$  mbar): membrane pumps, rotary pumps, scroll pumps, roots pumps
- Turbomolecular Pumps (from the mbar to about  $10^{-9}$  mbar )

2) **UHV pumping systems:** pumps that work at low pressure and, thanks to their efficiency, allow reaching/improving the ultra-high vacuum ( $10^{-6}$ - $10^{-11}$  mbar).

- Ion Pumps (from  $10^{-6}$  mbar to  $10^{-11}$  mbar)
- Getter Pump
- Titanium Sublimation Pump

# Rough pumps: membrane and rotary pumps

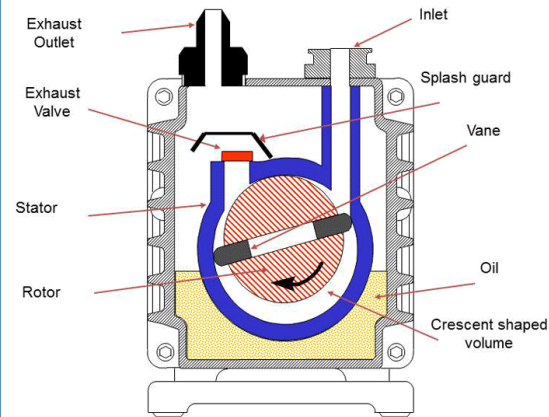


## Membrane

Combined movement of a diaphragm (plastic-rubber) and suitable valves (check, butterfly, flap valves)

Volume increased = fluid drawn into the chamber  
Volume decreased = fluid forced out

- **Dry pumps**
- Can handle gas and liquids
- The flow rate depends on the diaphragm diameter and its stroke length
- Ultimate vacuum is in the mbar (larger pumps can reach  $10^{-1}$  mbar)



## Rotary

Consists of vanes mounted to an eccentric rotor. The vanes rotate inside a cavity

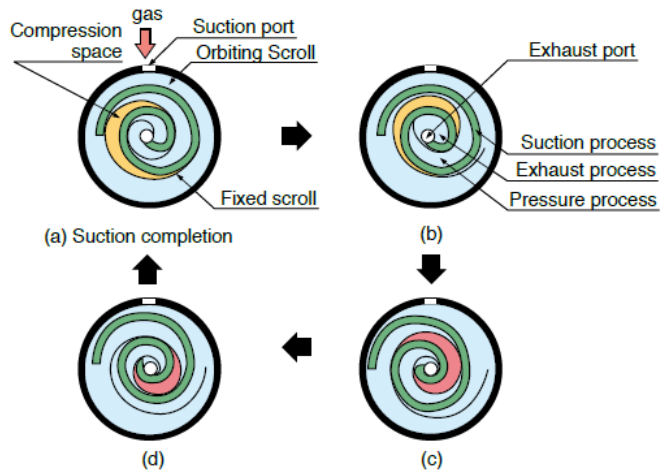
Vanes are sealed on all edges. The rotation generates a volume expansion (gas pumping)-reduction (exhaust release)

- **Oil pumps:** oil and gas are mixed inside the pump and separated externally
- Multiple stage pump can generate a good vacuum (down to  $10^{-3}$  mbar)
- Low efficiency but possibility to pump gas, gas + dust and water



# Rough pumps: scroll and roots pumps

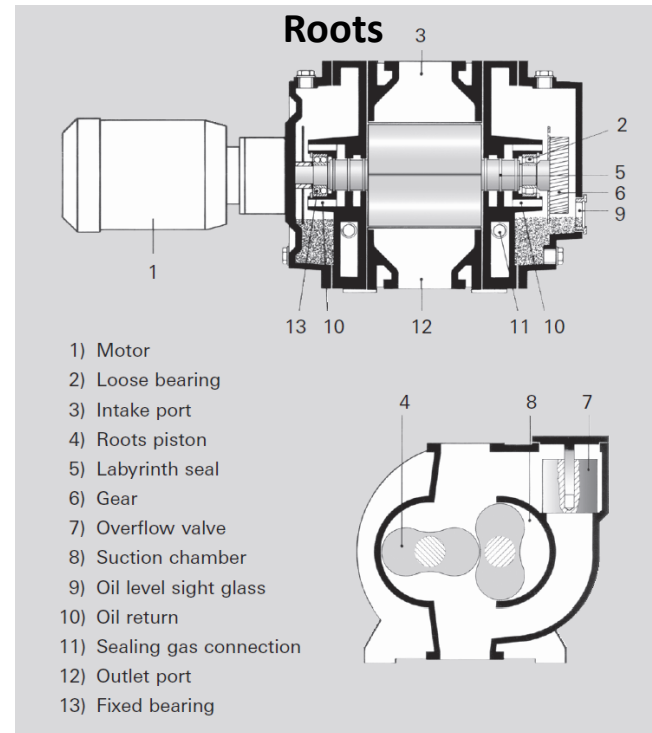
## Scroll



One of the scrolls is fixed, while the other orbits eccentrically without rotating. Compressing pockets of fluid form between the scrolls and are driven to the exhaust port

- **Dry pumps**
- High efficiency
- Small gas pulsation, less vibrations
- Difficult maintenance
- Ultimate vacuum is in the  $10^{-2}$  mbar range

## Roots



Two 8-shaped synchronously counter-rotating rotors rotate contactlessly (small gap) in a housing

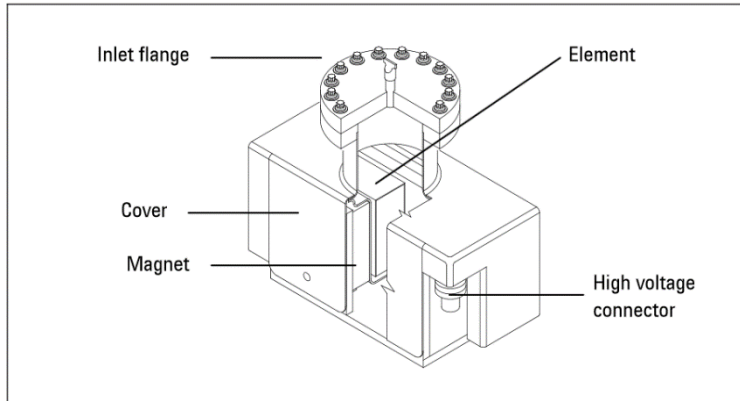
- **Dry pumps**
- Can generate a good vacuum (low  $10^{-2}$  mbar)
- No friction in the suction chamber, operation at high speed, large flow rate

# Turbomolecular pumps



- A turbomolecular pump is used to obtain and maintain **high vacuum**.
- These pumps work on the principle that gas molecules can be given momentum in a desired direction by repeated collision with a moving solid surface.
- A rapidly spinning fan rotor (50000-100000 rpm) 'hits' gas molecules from the inlet of the pump towards the exhaust in order to create or maintain vacuum.

## Ion pumps



- An ion pump is a **static pump** capable of reaching pressures as low as  **$10^{-11}$  mbar**
- Can be turned on only at pressures around (or less than)  $10^{-4}$  mbar
- A strong electrical voltage (typically 3–7 kV) is applied to the anode, producing free electrons. Electrons get caught by the magnetic field and rotate around it
- Electrons hit gas molecules ionizing them
- Positively charged molecules accelerates toward the cathode (grounded) at high velocity
- The cathode is sputtered and titanium compounds deposit on the anode
- The cathode acts as a getter (e.g. adsorbs inert gases)

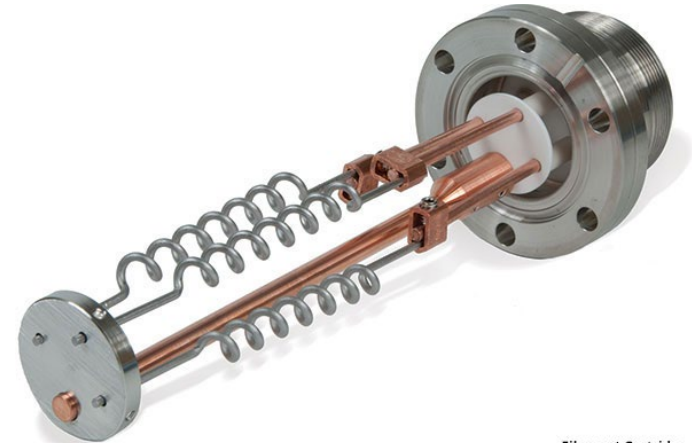
# Getter and TSP

## Non-evaporable getter



- Static pumps helping to establish and maintain ultra-high vacuum
- Porous alloys or powder mixtures of Al, Zr, Ti, V and Fe, forming stable compounds with active gases
- Can be placed in narrow/difficult to reach spaces (particle accelerators)
- Activated by annealing to  $>550$  K

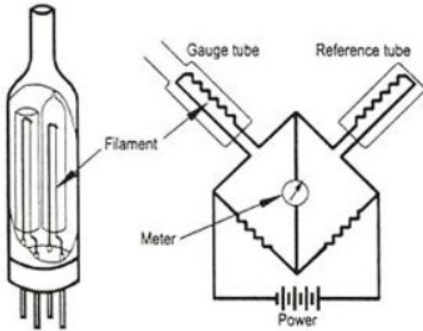
## Titanium sublimation



Filament Cartridge

- Static pump helping to refine the vacuum
- Titanium filament through which a high current (typically around 40 A) is passed periodically
- Titanium sublimates and coats the surrounding chamber walls
- Components of the residual gas in the chamber which collide with the chamber wall react with titanium to form stable, solid products

# Vacuum measurement



**Low vacuum:** Pirani (atm. pressure –  $10^{-4}$  mbar)

- Two Pt filaments are the arms of a Wheatstone bridge and heated to a constant temperature
- Residual gases conduct away part of the thermal energy of the measurement filament. The amount of electrical current needed to restore its temperature is converted to a pressure readout



**High vacuum:** cold cathode  
( $10^{-4}$ - $10^{-9}$  mbar)

- 2 electrodes: anode, cathode + permanent magnetic field (works like a ion pump!)

- The pressure is measured through a gas discharge in the gauge head. The gas discharge is obtained by applying a high voltage



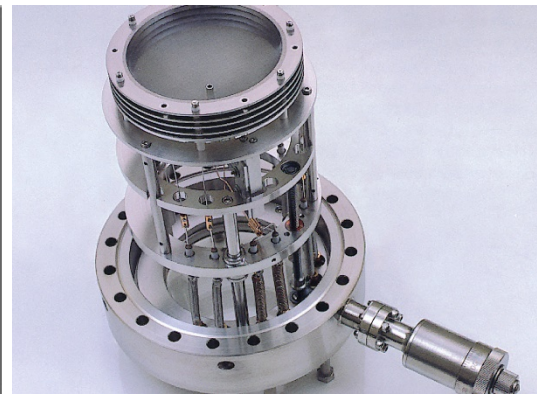
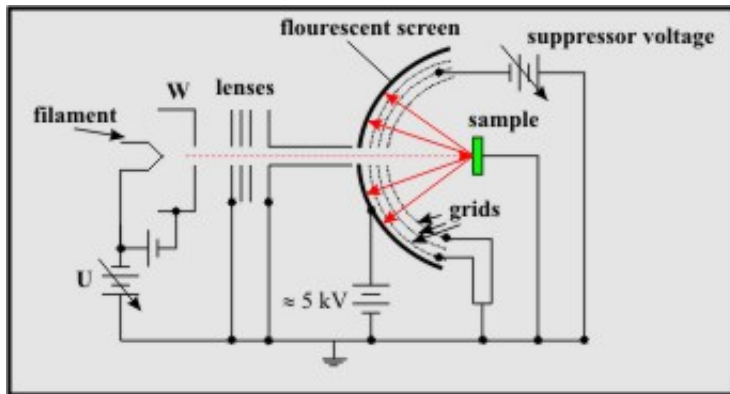
**High-Ultrahigh vacuum:** hot cathode  
( $10^{-4}$ - $10^{-11}$  mbar)

- 3 electrodes: filament, collector, grid
- The filament emits electrons, which are attracted to a polarized grid
- Residual gas molecules are ionized by the electrons and attracted by the collector. Pressure reading is determined by the electronics from the collector current.

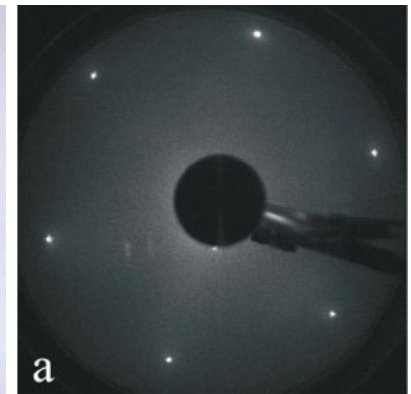
# Examples: vacuum techniques (surface science studies) – General description

## Electron-based techniques

- X-ray and UV photoelectron spectroscopy (XPS and UPS), Auger electron spectroscopy → 24.11.2020, h 15:45
- Low energy electron diffraction (LEED)



LEED instrument



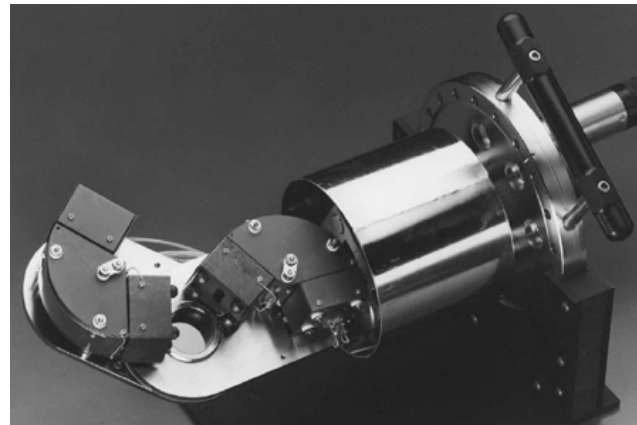
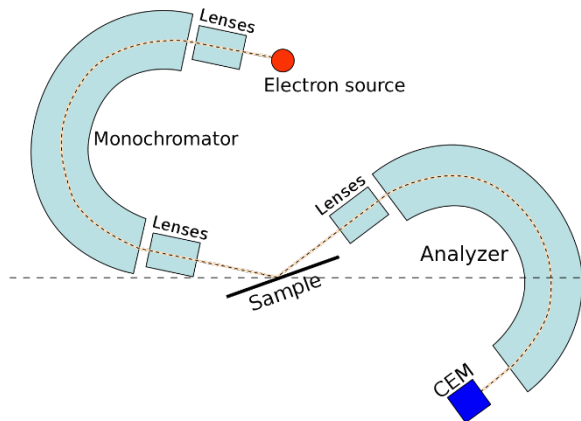
1x1 reconstruction  
Pt(111)

- Electron beam (20-2000 eV) hits a single-crystalline material
- Diffracted electrons are generated and hit a fluorescent screen: electrons impinging on an ordered surface are elastically scattered by it
- Information on the symmetry of the surface structure – surface sensitive

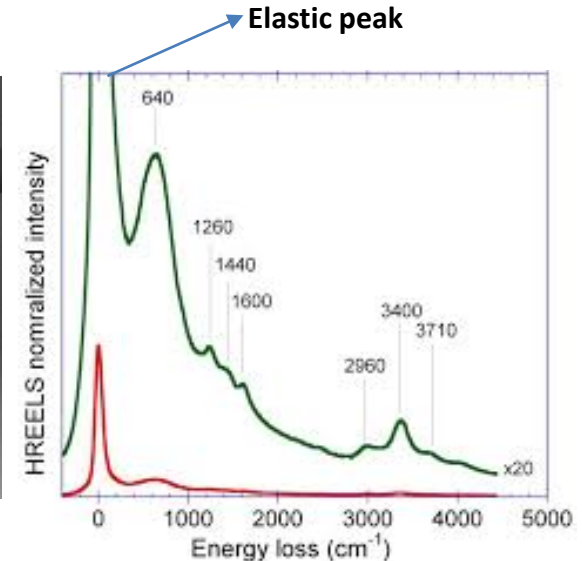
# Examples: vacuum techniques (surface science studies)

## Electron-based techniques

- High resolution electron energy loss spectroscopy (HREELS)



HREELS instrument



Example of EEL spectrum

- Electron beam ( $10^{-3}$ -10 eV) with known energy hits the surface of a material
- Electrons can excite the electronic structure of the sample or vibrational modes of adsorbates → energy loss of the electrons (inelastic scattering)
- The analyzer measures the energy of the scattered electrons and the energy losses are evaluated
- Surface properties of a sample learned from energy losses
- Selection rule: change of the dipole moment perpendicular to the surface
- Surface sensitive technique (a few nm)



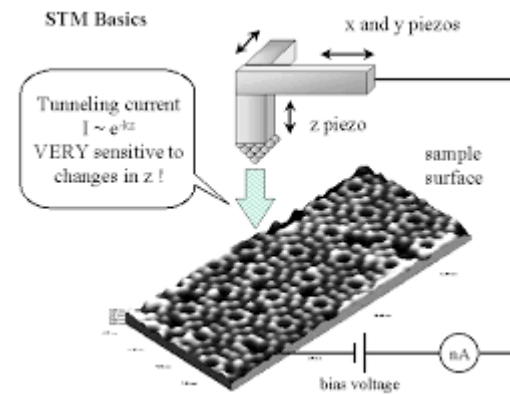
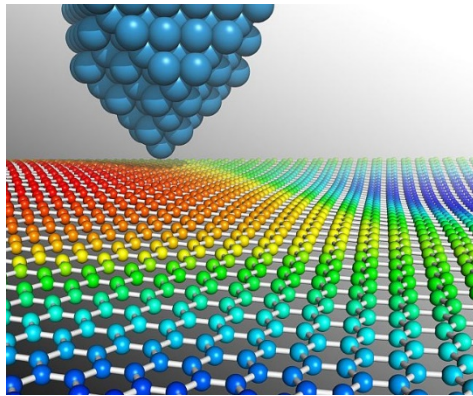
# Examples: vacuum techniques (surface science studies)

## Temperature Programmed techniques

- Temperature programmed desorption and reaction (TPD-TPR) → next topic

## Scanning probe microscopy techniques

- Scanning tunneling microscopy (STM)



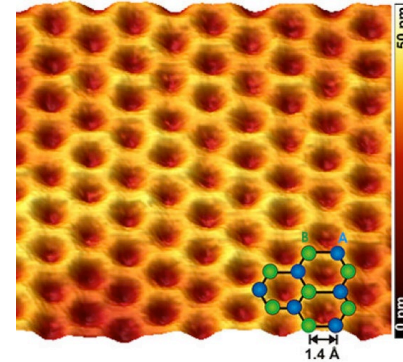
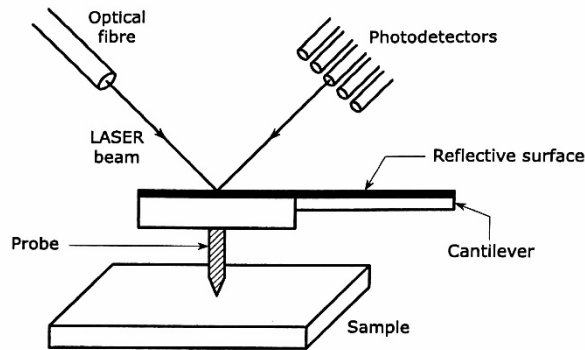
- A conductive tip is brought close to a surface and a bias is applied between the two
- Electrons can tunnel in the vacuum
- The measured tunneling current is a function of the tip position, applied bias and local density of states (LDOS)
- The tip is scanned across the surface while monitoring the current and plotted as an image



# Examples: vacuum techniques (surface science studies)

## Scanning probe microscopy techniques

- Atomic force microscopy (AFM)



- A cantilever with a sharp tip is used to scan the sample surface
- When the cantilever is brought close to the surface, forces (mechanical contact, van der Waals, capillary..) between the tip and the sample lead to a deflection of the cantilever
- The deflection is measured by means of a laser projected on the cantilever and deflected by it to a photodetector
- Can operate in contact mode (the tip drags the surface) or in non-contact mode (the cantilever oscillates at/near its resonant frequency and short contact forces experienced from the sample modify this vibration)

**TPD**

**Temperature Programmed Desorption**



# Temperature programmed desorption\*

Ultra high vacuum can be used to study the adsorption/reaction of molecules on a surface (monolayer formation time in UHV  $10^3$ - $10^6$  s). Discussion based on **Langmuir ad-(de-)sorption isotherm**

## Langmuir Adsorption-Desorption

- **Adsorption is localized (adsorbed particles are immobile)**
- **Substrate surface is saturated at  $\Theta = 1$  ML (all adsorption sites occupied)**
- **No interactions between the adsorbed particles**

## Kinetics

$$r_{\text{des}} = -\frac{d\Theta}{dt} = k_{\text{n}} \Theta^n$$

If  $k$  (rate constant) is described by an Arrhenius eq.:

$$k_{\text{n}} = v_n \cdot \exp\left(-\frac{\Delta E_{\text{des}}}{RT}\right)$$

The rate law is then referred to as the *Polanyi-Wigner* equation:

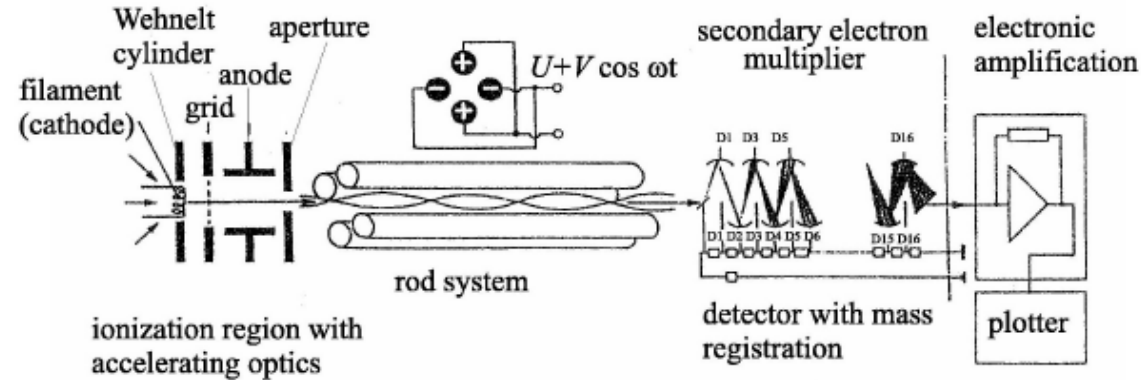
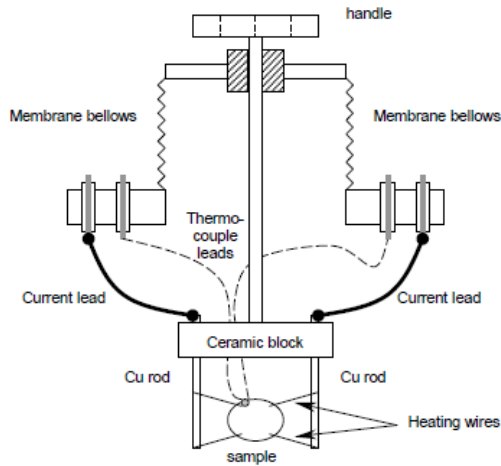
$$r_{\text{des}} = -\frac{d\Theta}{dt} = v_n \cdot \exp\left(-\frac{\Delta E_{\text{des}}}{RT}\right) \cdot \Theta^n$$

$v_n$ :	Pre-exponential factor
$n$ :	Desorption order
$\Theta$ :	Surface coverage
$E_{\text{des}}$ :	Activation energy for desorption

\*Resource for further reading: Temperature-Programmed Desorption (TPD). Thermal Desorption Spectroscopy (TDS), Sven L.M. Schroeder and Michael Gottfried, June 2002, available online.

# Temperature programmed desorption

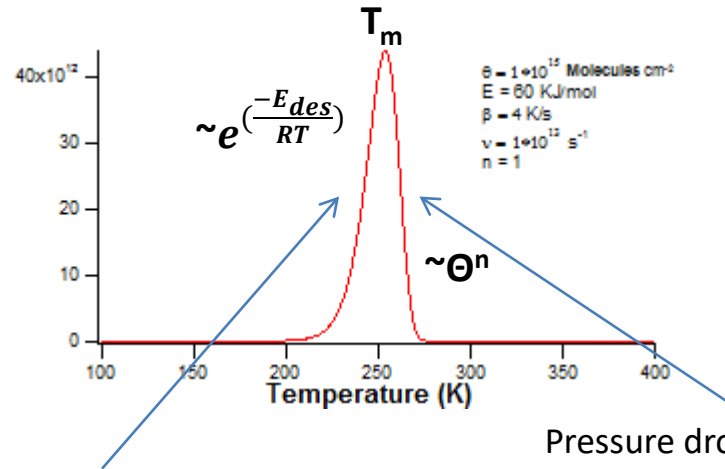
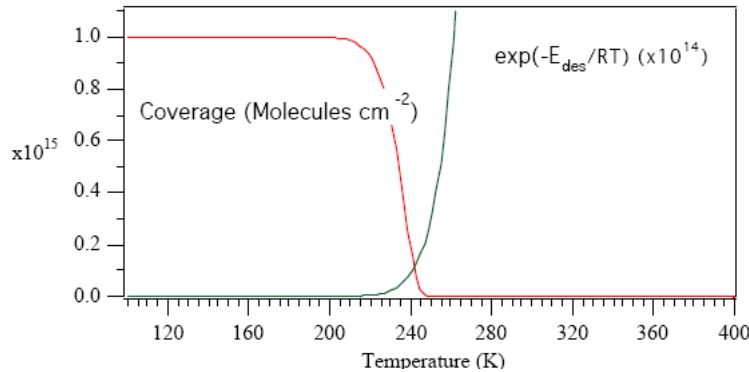
## A typical TPD experiment (UHV):



- Clean sample surface exposed to a precise amount of gas (usually measured in Langmuirs –  $1 \text{ L} = 10^{-6} \text{ Torr} \cdot \text{s}$ )
- Sample placed in front of a quadrupole mass spectrometer (QMS) and heated with a precise rate ( $\beta$ )
- The quadrupole acts as a filter, separating ions with different  $m/z$ , which are then collected
  - A typical spectrum shows the intensity of a specific  $m/z$  vs. temperature

# Temperature programmed desorption

If the pumping rate is faster than the desorption rate (no readsorption) a series of separated peaks can be recorded (each of them corresponding to a surface desorption process)



Initial increase is mainly determined by  $E_{des}$

Pressure drop gives information about the order of the desorption process

A TPD experiment can give important information:

- Heat of desorption
- Surface coverage (quantification of the monolayer)
- Surface reactivity (gas-substrate interaction, adsorption sites)
- Kinetics of desorption

# Temperature programmed desorption

Spectral interpretation is most commonly performed using the **Polanyi-Wigner equation**

In a TPD experiment  $\beta$  is the heating rate, defined as  $\beta = dT/dt = \text{const.}$  Thus  $dt = dT/\beta$  can be substituted in the equation to give

$$\frac{d\Theta}{dT} = -\frac{1}{\beta} v_n \cdot \exp\left(-\frac{\Delta E_{des}}{RT}\right) \cdot \Theta^n$$

When  $T = T_{\text{max}}$

$$\left. \frac{dr_{des}}{dT} \right|_{T=T_m} = 0; \quad r_{des} = -\frac{d\Theta}{dt} = -\beta \cdot \frac{d\Theta}{dT}; \quad \longrightarrow \quad 0 = \left. \frac{d^2\Theta}{dT^2} \right|_{T=T_m} = n \cdot \Theta^{n-1} \cdot \frac{d\Theta}{dT} + \Theta^n \cdot \frac{\Delta E_{des}}{RT_m^2}$$

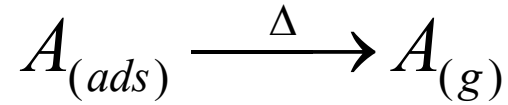
$$n \cdot \Theta^{n-1} \cdot \left[ -\frac{v_n \Theta^n}{\beta} \cdot \exp\left(-\frac{\Delta E_{des}}{RT}\right) \right] + \Theta^n \cdot \frac{\Delta E_{des}}{RT_m^2} = 0;$$

$$\Theta^n \cdot \frac{\Delta E_{des}}{RT_m^2} = \frac{n \cdot v_n \cdot \Theta^{n-1} \cdot \Theta^n}{\beta} \cdot \exp\left(-\frac{\Delta E_{des}}{RT_m}\right);$$

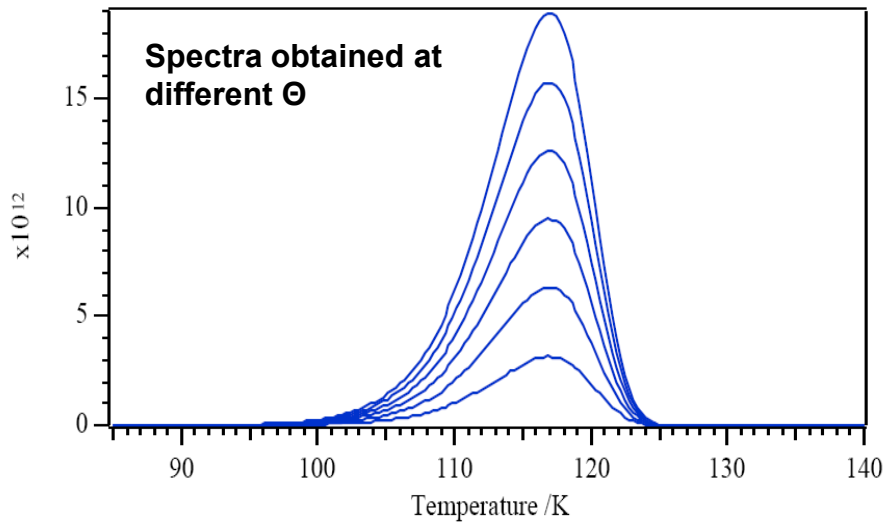
$$\frac{\Delta E_{des}}{RT_m^2} = \frac{n \cdot v_n \cdot \Theta^{n-1}}{\beta} \cdot \exp\left(-\frac{\Delta E_{des}}{RT_m}\right);$$

This equation can be used to obtain  $\Delta E_{des}$  from TPD spectra (see the next slides)

# First order kinetics (molecular)



$$-\frac{d\Theta}{dt} = \nu_n \cdot \Theta \cdot \exp\left(-\frac{\Delta E_{des}}{RT}\right); \quad \frac{\Delta E_{des}}{RT_m^2} = \frac{\nu}{\beta} \cdot \exp\left(-\frac{\Delta E_{des}}{RT_m}\right);$$



- The desorption peak areas depend on  $\Theta$
- The desorption peaks are asymmetric
- $T_m$  constant with increasing  $\Theta$
- $T_m$  increases with  $\Delta E_{des}$

# First order kinetics: approximate evaluation of $\Delta E_{des}$

In 1962 Redhead, assuming that activation parameters are independent of surface coverage and that desorption followed 1<sup>st</sup> order kinetics, derived a simple equation.\*

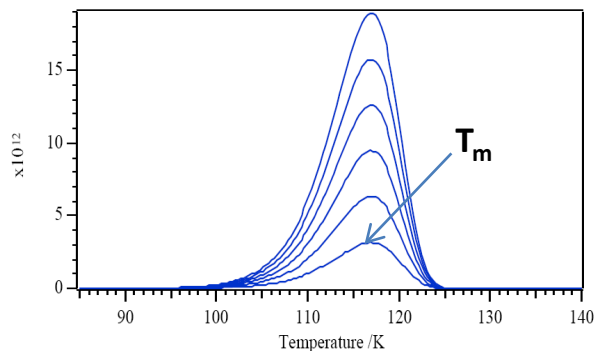
$$\frac{\Delta E_{des}}{RT_m^2} = \frac{\nu}{\beta} \cdot \exp\left(-\frac{\Delta E_{des}}{RT_m}\right);$$

Solving this equation for  $\Delta E_{des}$  gives:

$$\Delta E_{des} = RT_m \left[ \ln \frac{\nu \cdot T_m}{\beta} - \ln \frac{\Delta E_{des}}{RT_m} \right]$$

The second part in the brackets is small relative to the first, and can be approximated to 3.64 (error is less than 1.5% for  $10^8 < \nu/\beta < 10^{13} \text{ K}^{-1}$ )

- $T_m$  and  $\beta$  are determined experimentally
- The activation energy from a single desorption spectrum can be estimated using an approximate value for  $\nu$ .  $\nu = 10^{13} \text{ s}^{-1}$  is a commonly chosen value.



As an example: in this case  $T_m = 117 \text{ K}$ .

Assuming  $\nu = 1.0 \cdot 10^{13} \text{ s}^{-1}$  and  $\beta = 2 \text{ K/s}$

$$\Delta E_{des} = 29.5 \text{ kJ/mol}$$

\*P. A. Redhead, Vacuum 12, 203-211 (1962).

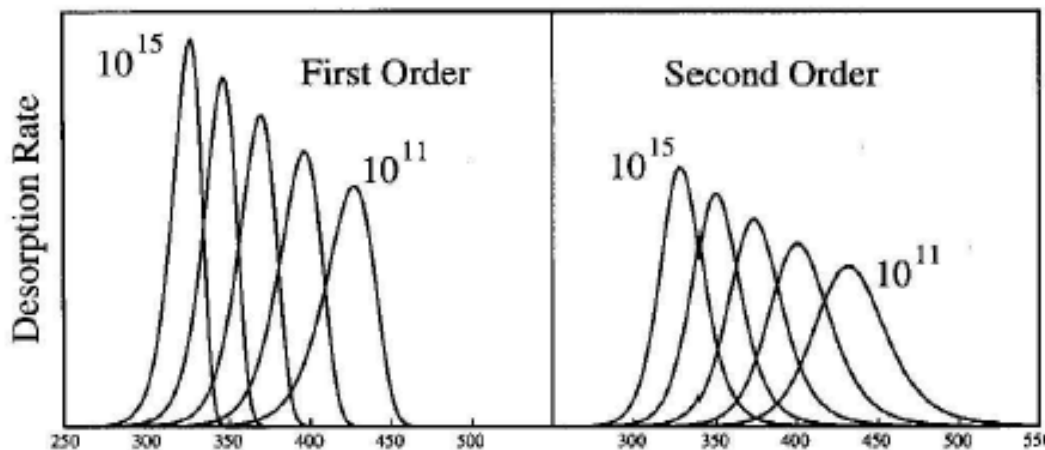


# First order kinetics: approximate evaluation of $\Delta E_{des}$ from curves having different $\beta$

A series of spectra for the same  $\Theta$  is acquired employing different  $\beta = dT/dt = \text{const.}$  From each spectrum, the temperature of the desorption rate maximum  $T_m$  is determined

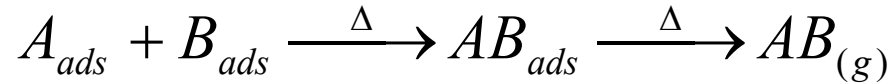
$$\frac{\Delta E_{des}}{RT_m^2} = \frac{\nu}{\beta} \cdot \exp\left(-\frac{\Delta E_{des}}{RT_m}\right); \quad \text{Taking the ln and rearranging..} \quad \ln \frac{T_m^2}{\beta} = \frac{\Delta E_{des}}{R \cdot T_m} + \ln \frac{\Delta E_{des}}{\nu \cdot R}$$

Plotting of  $\ln(T_m^2/\beta)$  vs.  $1/T_m$  for a series of  $\beta$  values provides  $\Delta E_{des}$  from the slope and  $\nu$  from the intercept with the ordinate



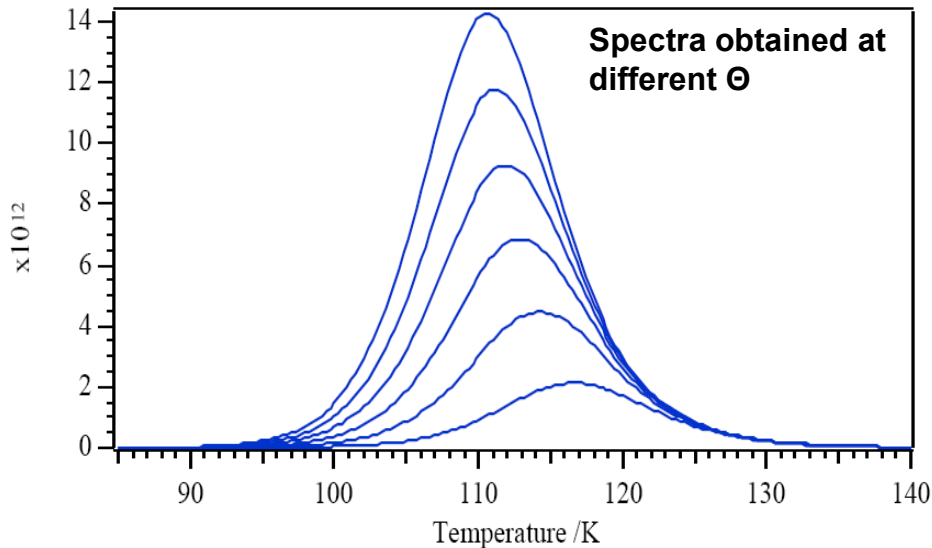
*Variation of the heating rate*  
 $\Theta_0 = 0.67, n = 1, 2,$   
 $\nu_n/\beta_H = 10^{11} \dots 10^{15},$   
 $E_d = 100 \text{ kJ/mol.}$

## Second order kinetics (recombinative desorption)



$$-\frac{d\Theta}{dt} = \nu_n \cdot \Theta^2 \cdot \exp\left(-\frac{\Delta E_{des}}{RT}\right);$$

$$\frac{\Delta E_{des}}{RT_m^2} = \frac{2 \cdot \nu_n \cdot \Theta}{\beta} \cdot \exp\left(-\frac{\Delta E_{des}}{RT_m}\right);$$



- $T_m$  shifts with increasing  $\Theta$
- Characteristic nearly symmetric peak shape with respect to  $T_m$
- $\Theta(T_m)$  is a half of the value before desorption

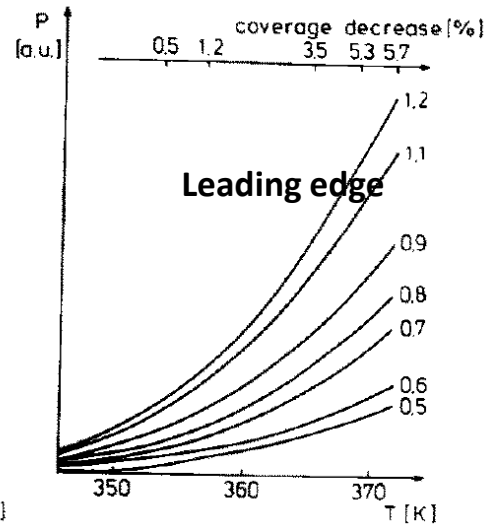
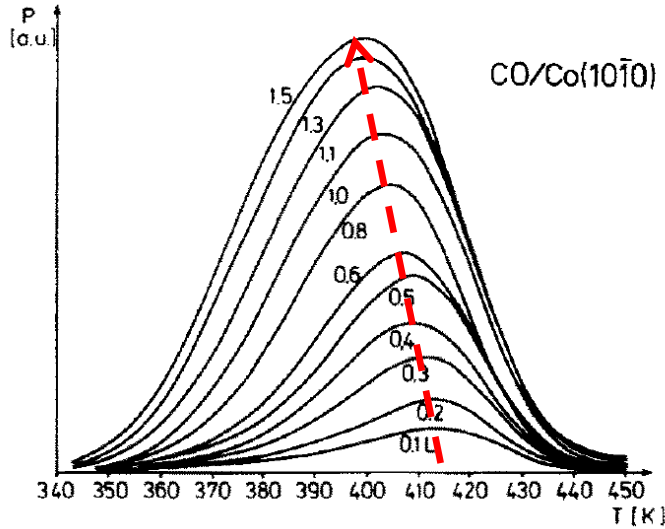
dividing by the units and rearranging we obtain:

$$\ln \frac{T_m^2}{\beta} = \frac{\Delta E_{des}}{R \cdot T_m} + \ln \frac{\Delta E_{des}}{\nu \cdot R \cdot \Theta}$$

Plotting the  $\ln(T_m^2/\beta)$  vs.  $1/T_m$  for a series of  $\beta$  values provides  $\Delta E_{des}$  from the slope and (if  $\Theta$  is known)  $\nu$  from the intercept with the ordinate

# Leading edge analysis

But the activation parameters often depend on the coverage and temperature!



Increasing  $\Theta$ ,  $T_m$  shifts negatively due adsorbate-adsorbate interactions

## Habenschaden and Küppers leading edge method\*

- Leading edge:  $\Theta$  almost unchanged
- The rate of desorption is evaluated from each single leading edge

$$r_{\text{des}} = v_n \cdot \exp\left(-\frac{\Delta E_{\text{des}}}{RT}\right) \cdot \Theta^n \quad \longrightarrow \quad \ln(r_{\text{des}}) = -\frac{\Delta E_{\text{des}}}{RT} + \ln(v_n) + n \ln \Theta$$

- $\ln(r_{\text{des}})$  plotted vs.  $1/T$ . The slope gives  $\Delta E_{\text{des}}$  and the intercept with y gives  $v$

\*E. Habenschaden, J. Küppers, Surf. Sci. 138, L147 (1984).

# An example of TPD applied to the study of a catalytic reaction

1 / VOL. 1, NO. 2  
THE CHEMICAL EDUCATOR  
© 1996 SPRINGER-VERLAG NEW YORK, INC.

ISSN 1430-4171  
<http://journals.springer-ny.com/chedr>  
10.1007/s00897060028a

## Laboratories and Demonstrations

# A Laboratory Study of Heterogeneous Catalysis in Ultrahigh Vacuum

**M. M. WALCZAK**  
St. Olaf College  
1520 St. Olaf Ave.  
Northfield, MN 55057-1098

**H.R. BURKHOLDER and P. A. THIEL\***  
Iowa State University  
Ames, IA 50010  
[thiel@ameslab.gov](mailto:thiel@ameslab.gov)

## Carbon monoxide oxidation on a Pt foil

The purpose of the experiment is to determine which mechanism operates in the catalytic oxidation of carbon monoxide over platinum foil. Briefly, the Langmuir-Hinshelwood (LH) mechanism [2] requires adsorption of both species involved in the reaction. The Eley-Rideal (ER) mechanism [2] involves adsorption of only one reactant with subsequent reaction by impingement of the other from the gas phase. The goal is to distinguish between these two mechanisms.

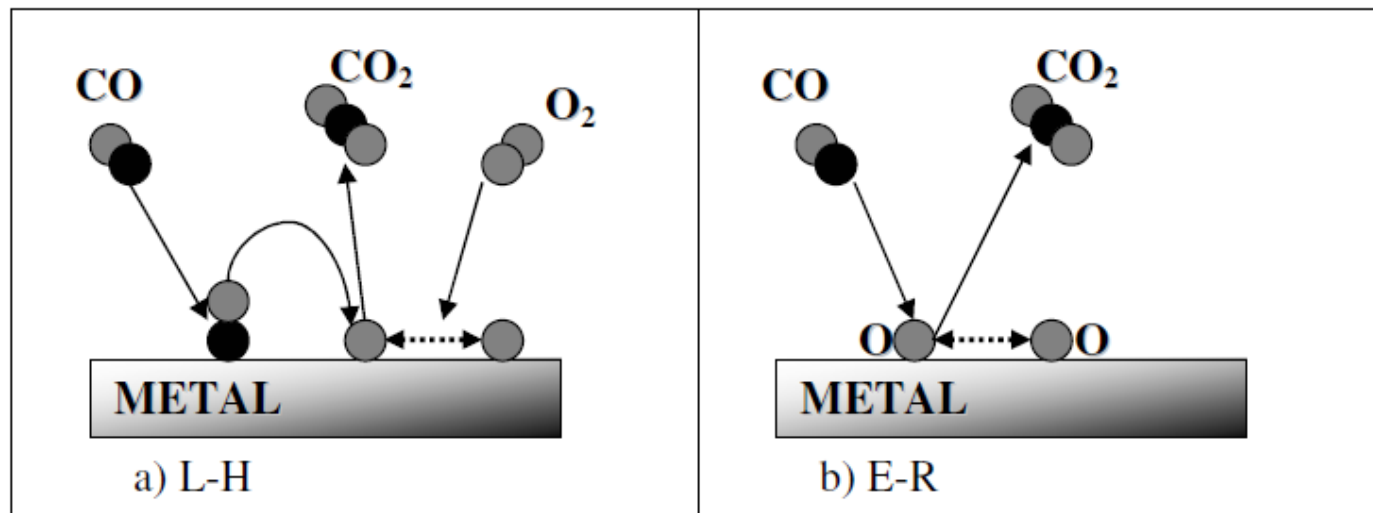
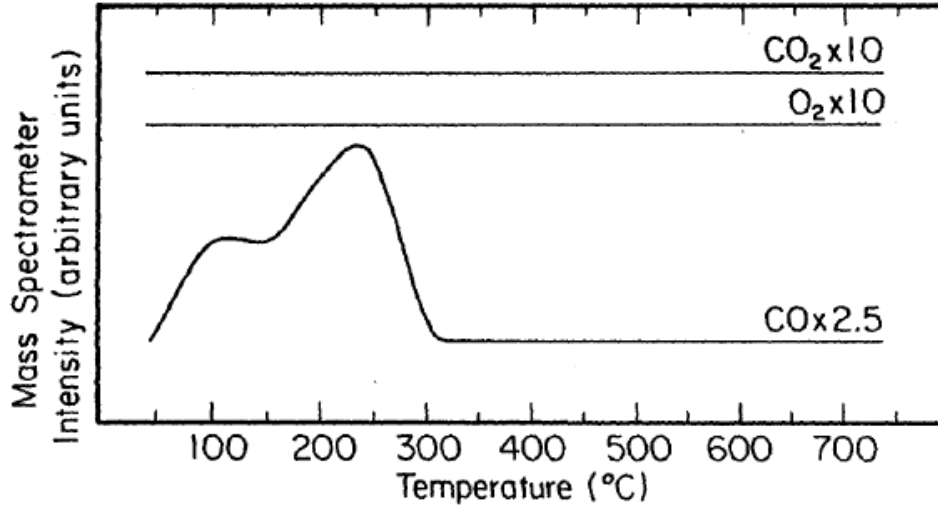


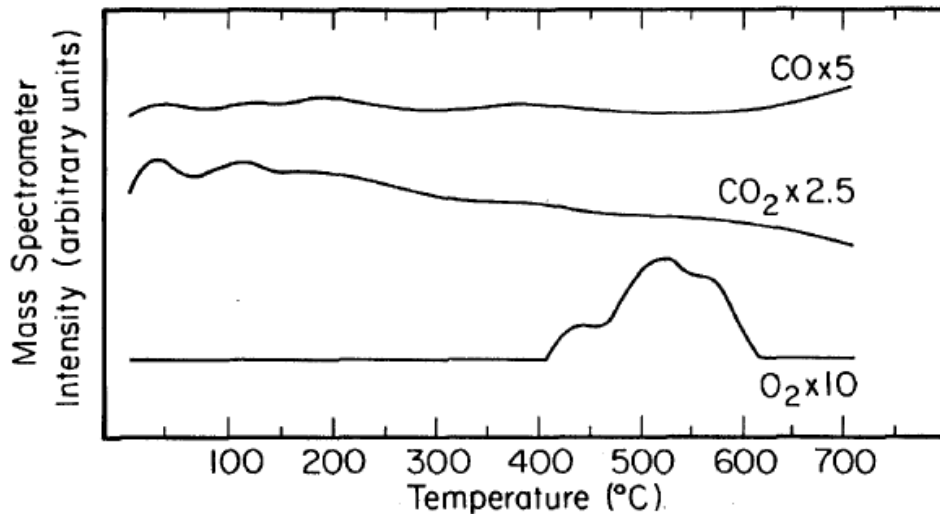
*Figure 2.2: Schematic representation of the Langmuir-Hinshelwood mechanism (a) and the Eley-Rideal mechanism (b) for the catalytic oxidation of CO. Dark balls correspond to the carbon atoms and grey balls correspond to the oxygen atoms.*

# CO and O<sub>2</sub> desorption

Procedure: 50 L of gas dosed on the clean foil at RT. Sample heated from RT to 700°C with  $\beta=10$  K/s



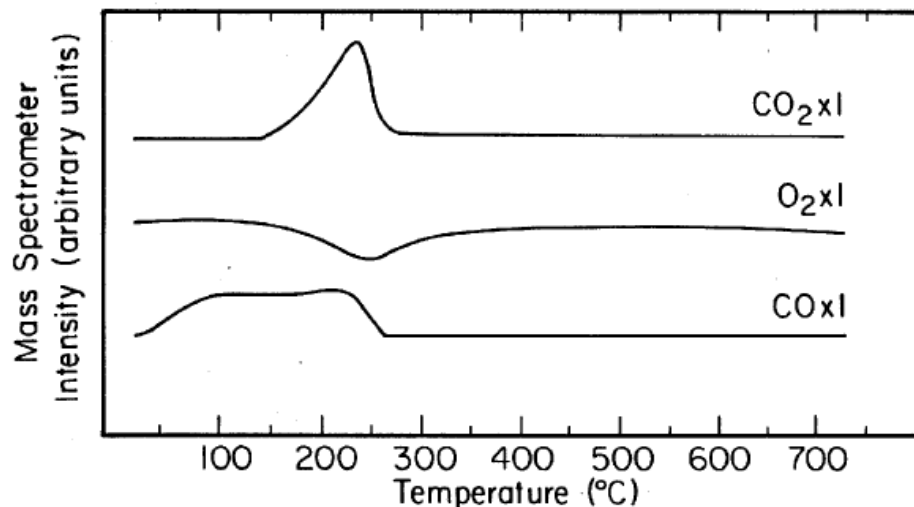
- Molecular adsorption (first order)
- Two main desorption peaks (a foil is polycrystalline) at ca. 110 and 225°C



- Dissociative adsorption (recombinative desorption process)
- Multiple desorption peaks at higher temperature than for CO (larger  $\Delta E_{\text{des}}$ )

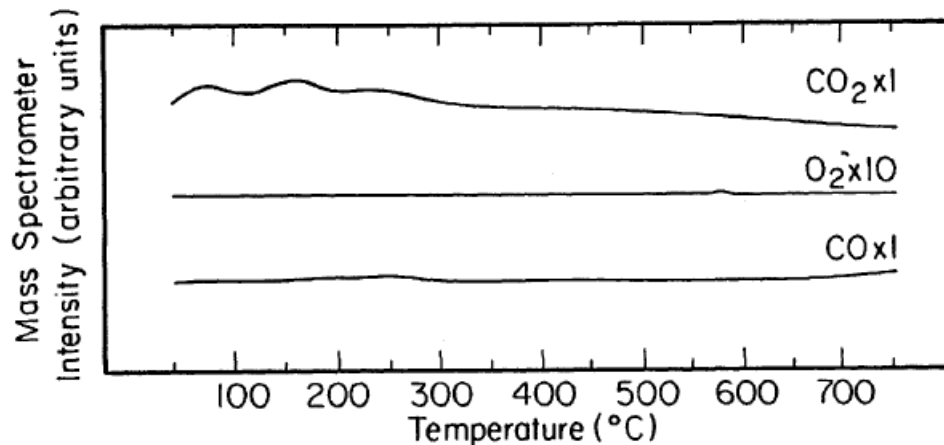
# Temperature programmed reaction (TPR)

Procedure: 50 L of CO dosed on the clean foil at RT. Sample heated from RT to 700°C with  $\beta=10$  K/s while flowing  $3 \cdot 10^{-7}$  Torr of  $O_2$ .



- Sample surface saturated with CO
- CO desorption peaks intensity decreases
- As the CO starts to desorb, the partial pressure of  $O_2$  decreases and the signal of  $CO_2$  increases

Procedure: 50 L of  $O_2$  dosed on the clean foil at RT. Sample heated from RT to 700°C with  $\beta=10$  K/s while flowing  $3 \cdot 10^{-8}$  Torr of CO.



- Sample surface saturated with  $O_2$
- $CO_2$  is produced immediately, but its signal goes down above 300°C
- **$CO_2$  production correlated with CO desorption**

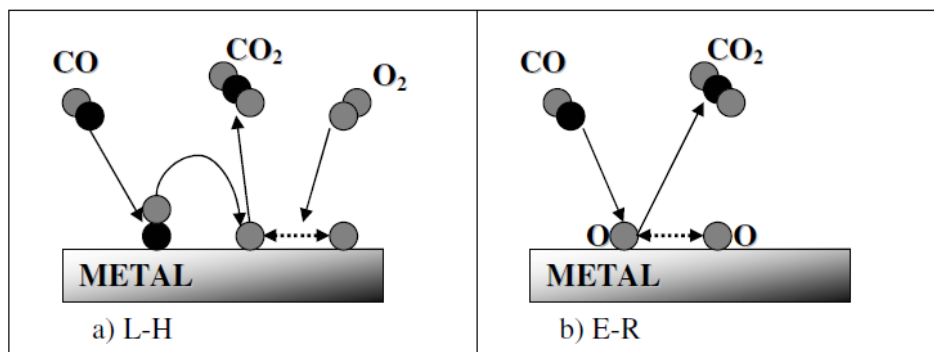


Figure 2.2: Schematic representation of the Langmuir-Hinshelwood mechanism (a) and the Eley-Rideal mechanism (b) for the catalytic oxidation of CO. Dark balls correspond to the carbon atoms and grey balls correspond to the oxygen atoms.

**In case of E-R mechanism the reaction should start immediately after introducing one of the reagents (in the presence of the other adsorbed)**

- In both TPR experiment CO<sub>2</sub> production correlates with the presence of both reagents on the sample surface
- TPR performed after CO pre-adsorption clearly demonstrates competition between the reagents for the adsorption sites (especially reaction at high temperature). CO is blocking the adsorption sites (poisoning effect), and some energy (temperature) is required to remove part of it and allow oxygen to adsorb and split
- TPR performed after O<sub>2</sub> pre-adsorption clearly demonstrates that adsorbed CO is necessary for CO<sub>2</sub> formation (no more CO<sub>2</sub> formed above 300°C)

These model experiments support the hypothesis that a L-H mechanism operates, in good agreement with the literature





# XPS

## X-ray Photoelectron Spectroscopy

Resource for further reading: *Surface Analysis by Auger and X-ray Photoelectron Spectroscopy*, D. Briggs, J.T. Grant, eds., IM Publications and SurfaceSpectra Ltd., 2003  
*Photoelectron Spectroscopy, Principles and Applications*, S. Hüfner, eds. Springer-Verlag Berlin Heidelberg 1995,1996,2003.

# What is XPS?

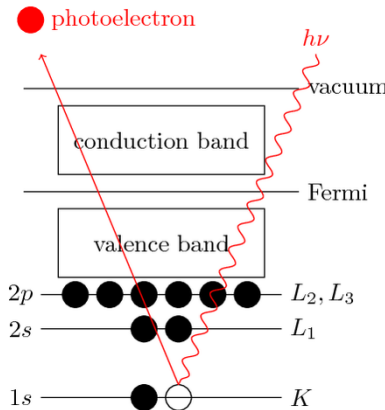
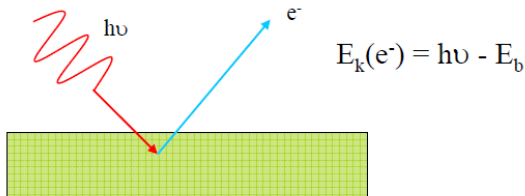
Nobel prize (physics) 1981



© 2000 by John Wiley & Sons, Ltd  
Kai Siegbahn

**XPS**  
X-ray photoelectron spectroscopy

**ESCA**  
Electron spectroscopy for chemical analysis



Nobel prize (physics) 1921



**Photoelectric Effect**  
Albert Einstein

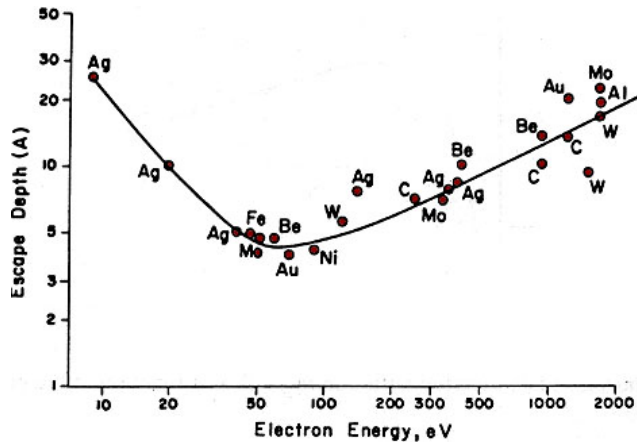
$$h\nu + E_i = E_k(e^-) + E_f$$

$$h\nu - E_k(e^-) = E_f - E_i = E_b$$

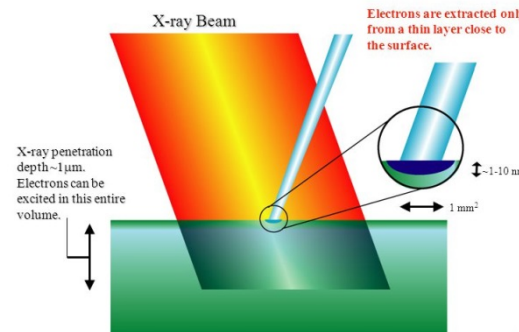
Binding energy!

The binding energies are characteristic of **specific electron orbitals in specific atoms**

- XPS lines are identified by the shell from which the electron is emitted



- Photoelectrons can escape only a few nm (this depends on their KE)

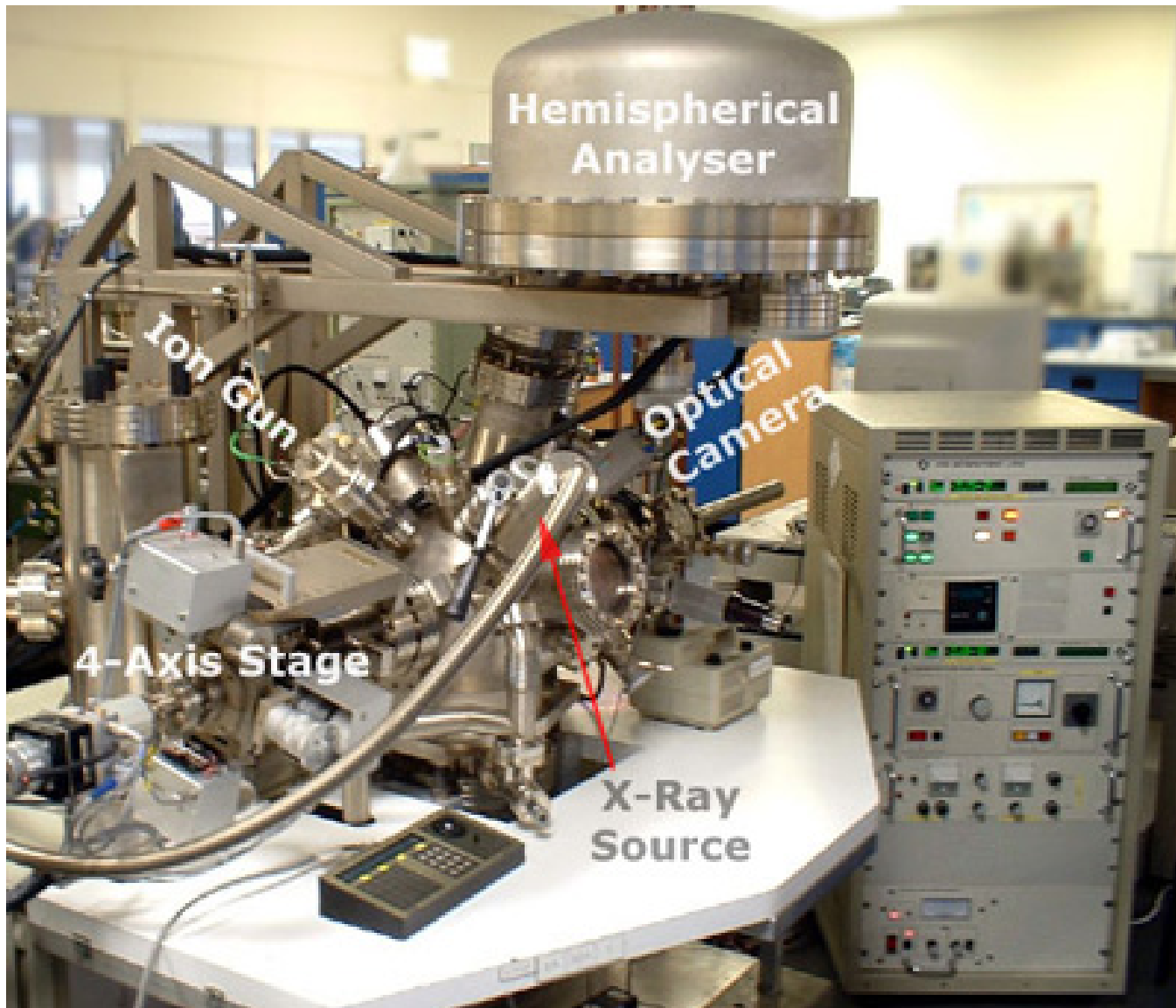


**Surface sensitive!**

## XPS in a nut-shell

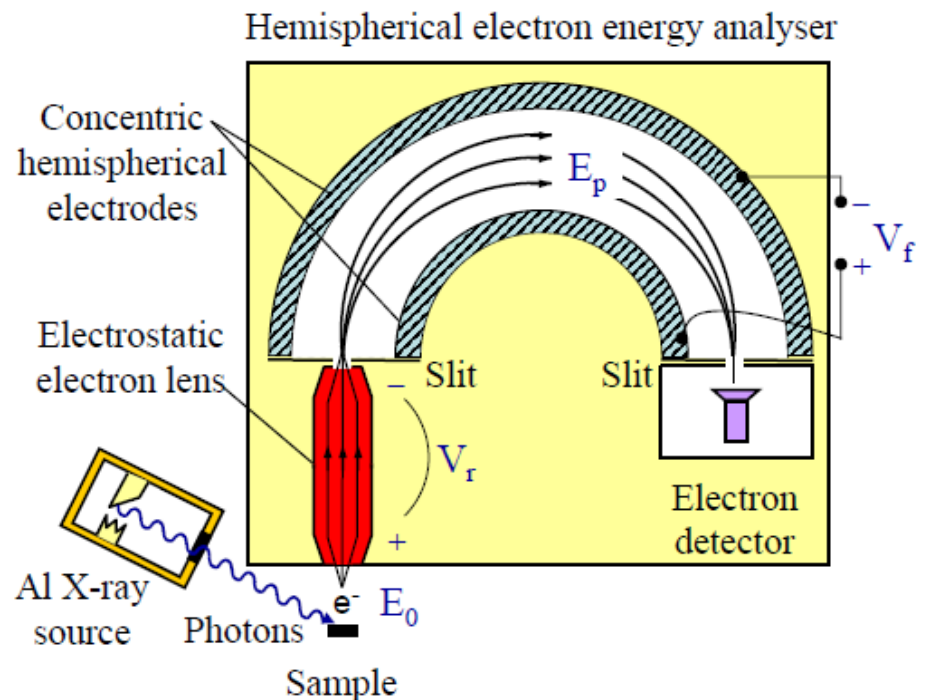
- X-ray photoelectron spectroscopy (XPS) is a classical method for the semiquantitative analysis of surface composition
- It is also referred to as Electron Spectroscopy for Chemical Analysis (ESCA)
- It is based on the photoelectric effect, i.e., emission of electron following excitation of core level electrons by photons
- It is surface sensitive because of the low inelastic mean free path of electrons
- An XPS setup consists of a X-ray source, a sample chamber and an electron analyzer
- XPS requires a source of X-rays, i.e., either from a lab-based anode or from a synchrotron
- Traditionally, XPS works only in ultrahigh vacuum because of scattering of electrons in gases
- XPS can also be performed in the mbar pressure range

This is a lab based XPS instrument

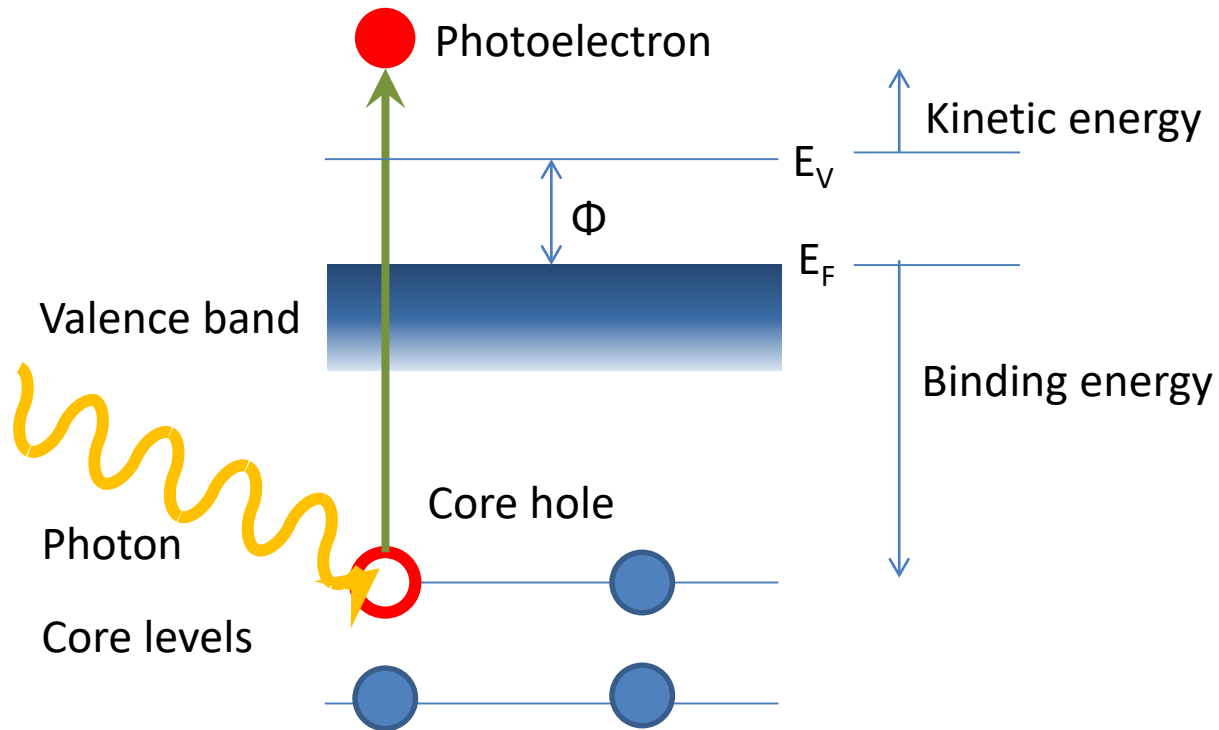


# Electron energy analyzer

- The most often used type of electron kinetic energy analyzers is composed of an **electrostatic lens** and a **hemispherical analyzer**
- Electrostatic lens decelerates electrons to a **fixed (pass) energy** in the range of a few to 100 eV and at the same time focusses them on an entrance slit of the hemispherical analyzer
- Electrons **travel between two concentric hemispheres with a constant potential difference** and reach a detector with one dimension aligning a small kinetic energy range
- A spectrum is obtained by **sweeping the lens electric field** to cover specific kinetic energy ranges of the photoelectrons
- Operation of an electron analyzer requires high vacuum to avoid scattering losses of electrons and to protect the detector



# The photoemission process



$$KE = h\nu - BE - \Phi \quad \text{for a solid}$$

$$KE = h\nu - IP \quad \text{for a gas}$$

$\Phi$  : photoelectric workfunction

# Fate of core hole

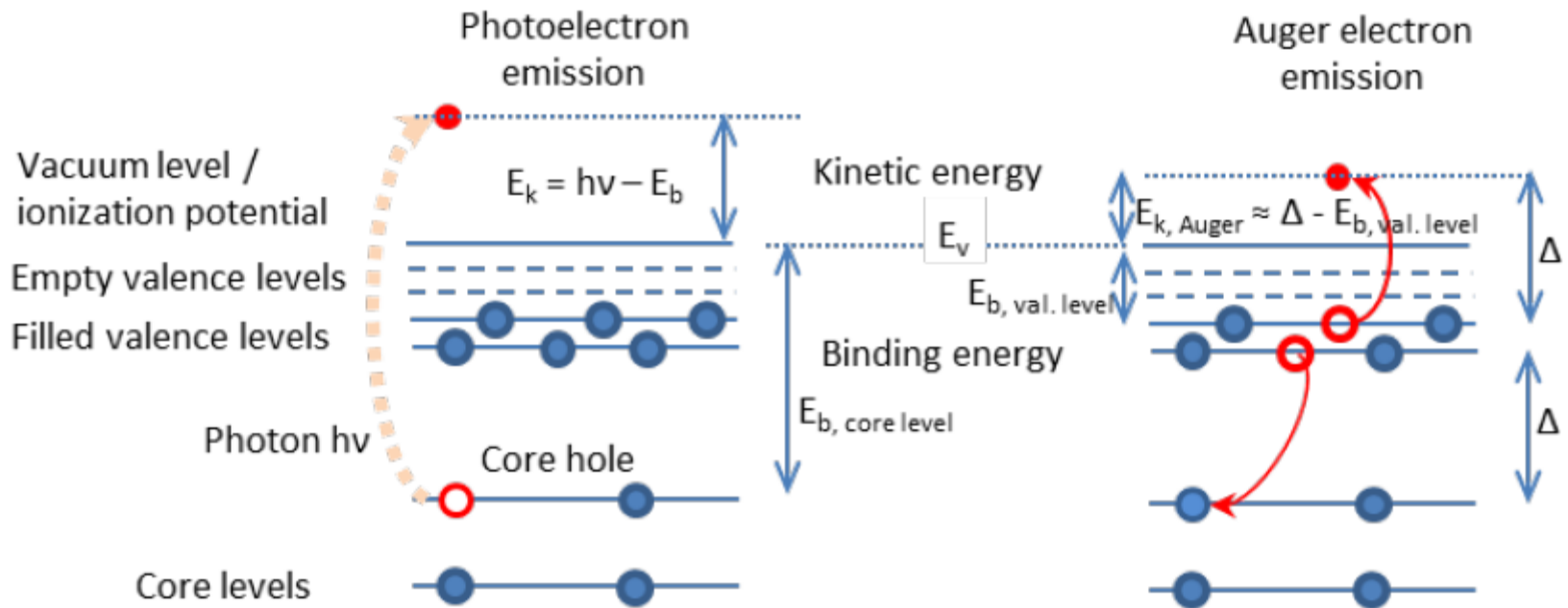
Photoemission



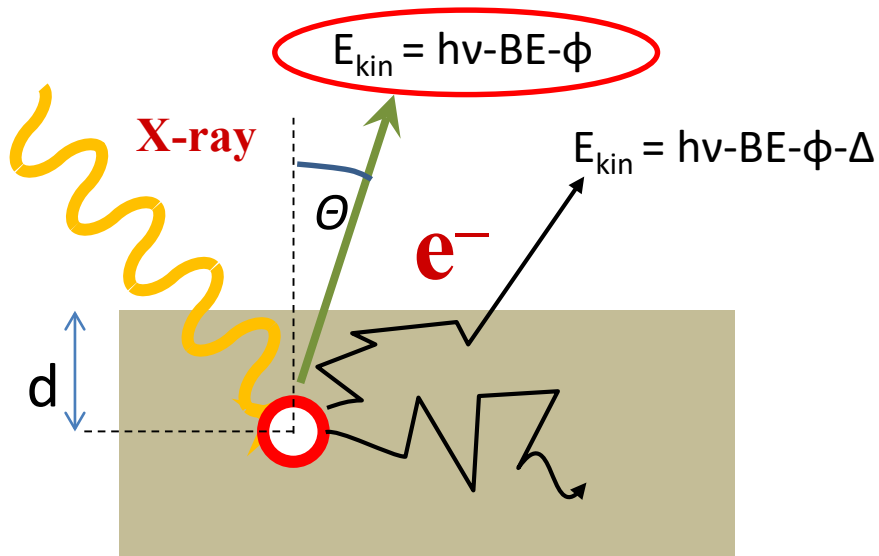
Relaxation



Auger electron emission  
or  
X-ray fluorescence



## Why is XPS surface sensitive? XPS probe depth



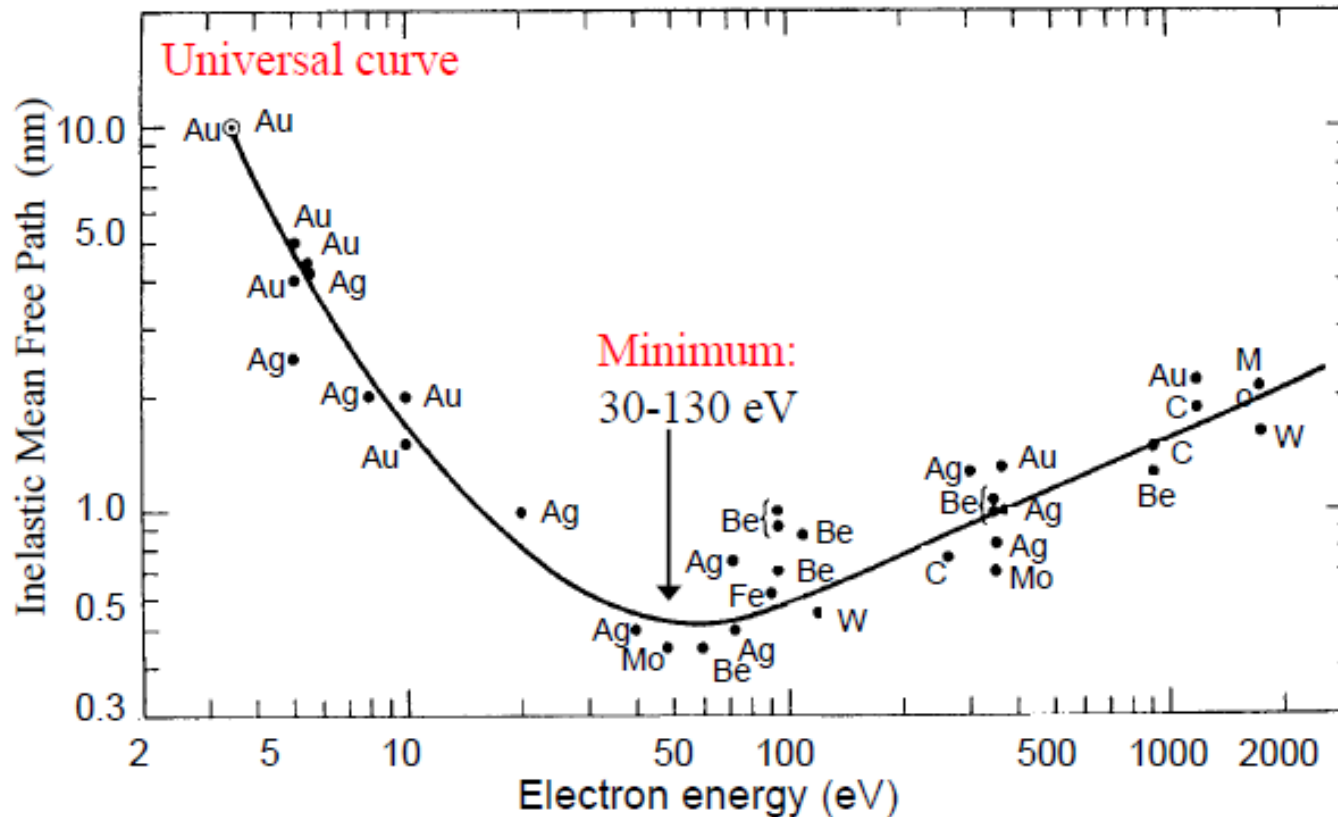
Contribution of atom in depth  $d$  to PE peak:

$$I = I_0 \exp\left(\frac{-d}{\lambda \cos \theta}\right)$$

- X-ray photons can penetrate  $\mu\text{m}$  but...
- Only photoelectrons from the first layers can escape without energy loss
- Inelastic mean free path ( $\lambda$ ) and probing depth strongly depends on the kinetic (and thus photon) energy
- Depth profiles can be obtained either by varying the incident photon energy (tunable x-ray source) or by varying the detection angle ( $\theta$ )
- Contribution to the photoelectron signal from atoms below the surface decreases exponentially
- In normal emission 95% of the signal comes from a  $3\lambda$  depth



# Electron inelastic mean free path



**Rule of thumb:**

$h\nu=1000$  eV

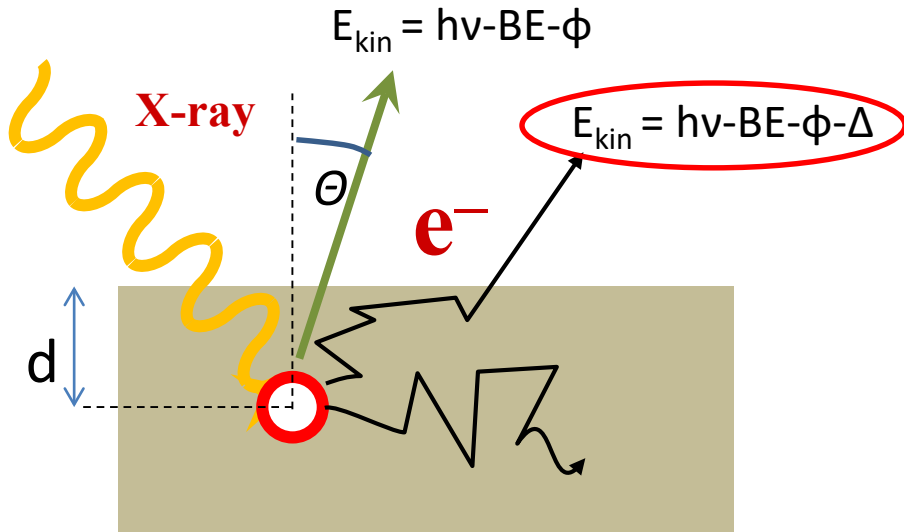
$\lambda_{\text{mfp}}$ :

5-10 Å metals

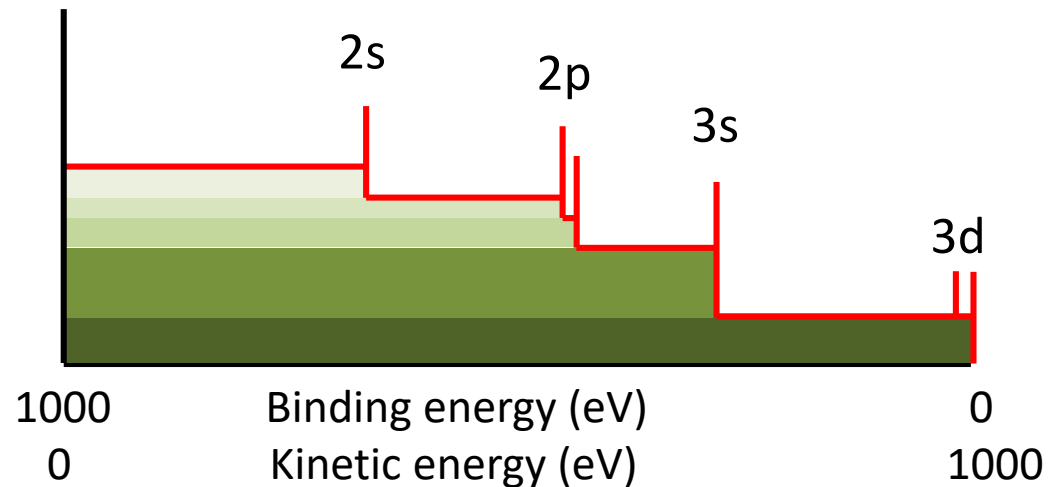
15-40 Å oxides

15-30 Å polymers

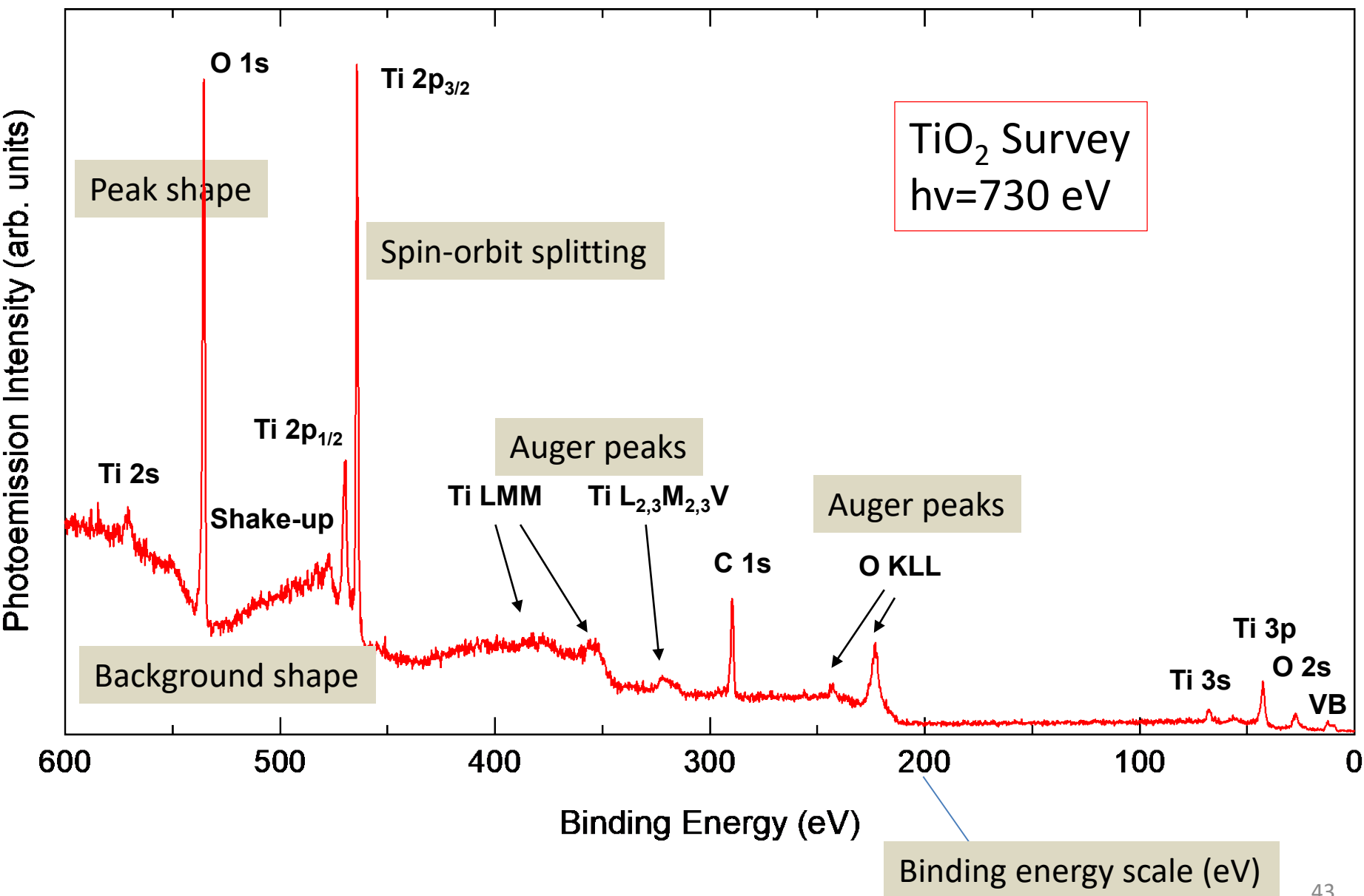
# Inelastic background



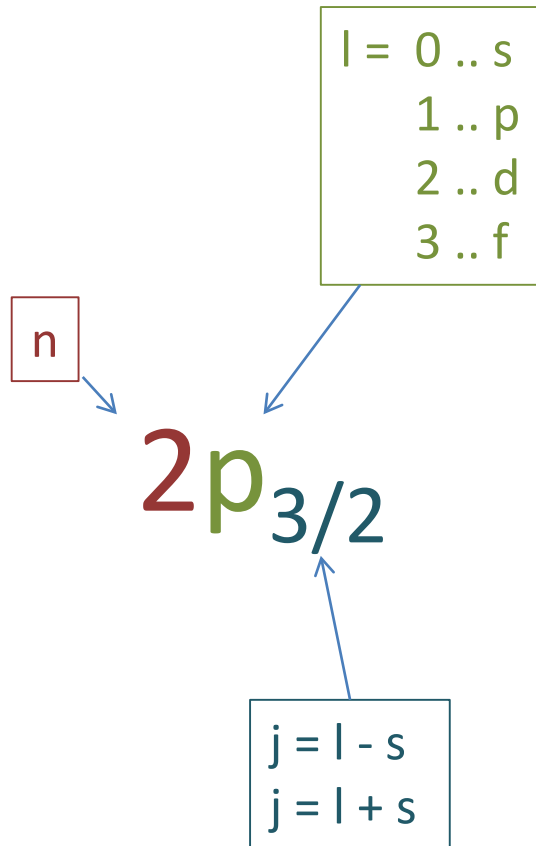
- Photoelectrons from deeper layers lose part of their energy (inelastic collisions) and are emitted with reduced KE ( $> BE$ )
- XPS spectra show characteristic "stepped" background (intensity of background towards higher BE of photoemission peak is always larger than towards lower BE)



# A photoelectron spectrum in more detail



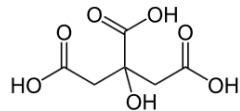
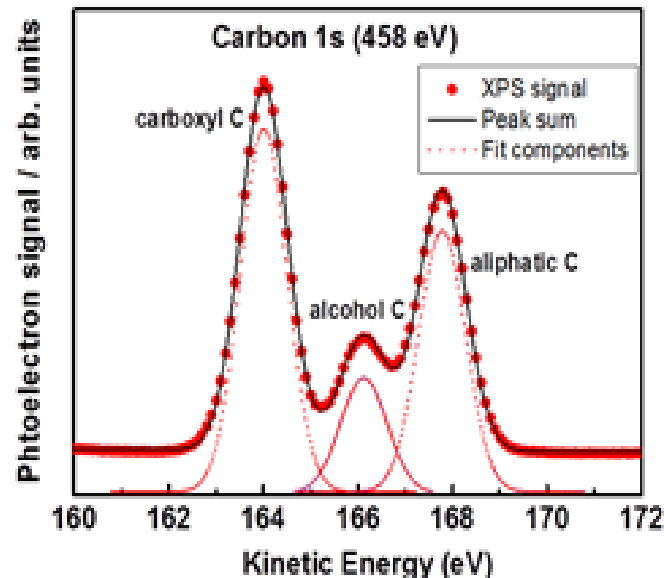
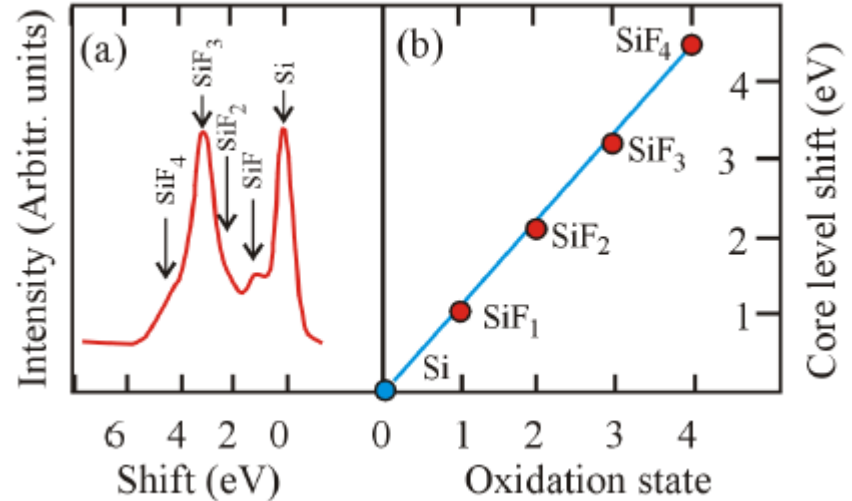
## Spin-orbit splitting



- $n$ : principal quantum number
- $l$ : orbital angular momentum quantum number
- $s$ : spin angular momentum quantum number
- $j = |l \pm s|$ : total angular momentum quantum number
- For  $l = 0$ , **s levels** are singlets, no splitting
- For  $l > 0$ , **p,d,f levels** give rise to **doublets**. The spin angular momentum of electrons left in an orbital couple with the angular momentum vector
- The degeneracy  $2j + 1$  determines the possibility for parallel and anti-parallel pairing
- The ratio between the degeneracies ( $R$ ),  $(2j_+ + 1)/(2j_- + 1)$ , determines the relative peak ratio of the two peak components.
- $\Delta E$  between two components = spin orbit splitting.
- Magnitude of spin-orbit splitting increases with  $Z$  and decreases with distance from nucleus (same energy level,  $\Delta E$  increases with decreasing  $l$ )

# Core level chemical shifts

- Position of orbitals in atom is sensitive to its **chemical environment**
- **Chemical shift** correlated with *overall charge* on atom (more positive charge = increased BE)
  - number of substituents
  - substituent electronegativity
  - formal oxidation state (depending upon ionicity/covalency of bonding)
- Chemical shift analysis is a powerful tool for chemical composition, functional group and oxidation state analysis

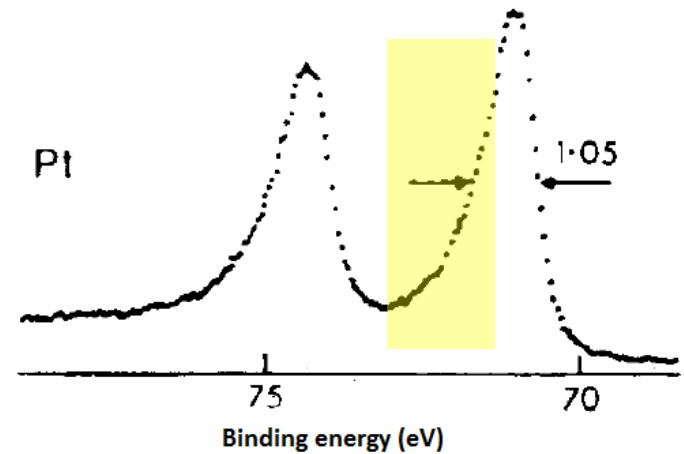


Citric acid

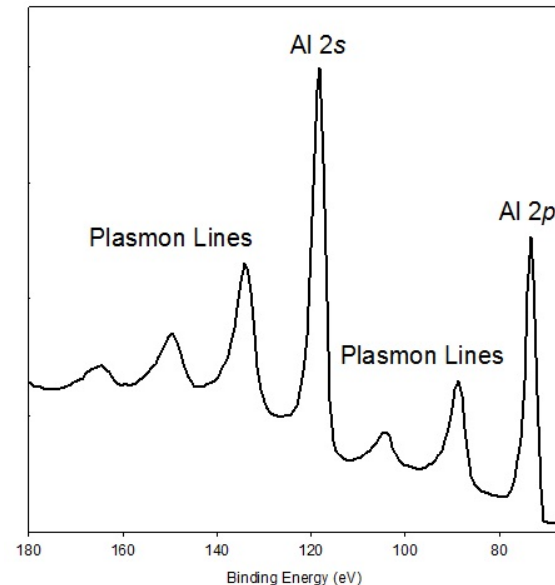
## Secondary structure of a spectrum

Interaction of the photoemitted electron (along its trajectory) and the remaining electrons:  
**final state effects (satellite peaks)**

- **Shake-up.** An electron of the VB can be excited. The energy of this excitation will be deducted from the kinetic energy of the photoelectron. Relevant in metals, in which the valence and conduction bands overlap, empty states are available at very low excitation energies

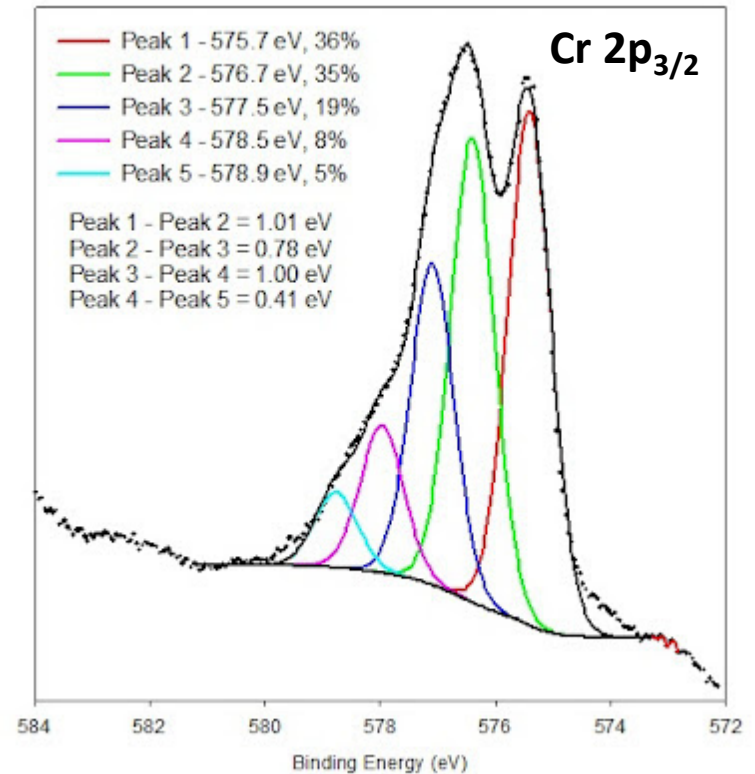


- Simultaneous excitation of a specific wave mode in the sample (e.g. **surface plasmons**). The kinetic energy loss is  $h\omega_s$  ( $\omega_s$  is the plasmon frequency), and will repeat at multiples of  $\omega_s$



## Secondary structure of a spectrum

- **Multiplet splitting.** Arises when an atom contains **unpaired electrons** (e.g.  $\text{Cr}^{3+}$ ,  $3p^6 3d^3$ ). During the photoemission process, there can be coupling between the unpaired electron in the core with the unpaired electrons in the outer shell. This can create a number of final states, which will be seen in the photoelectron spectrum as a multi-peak envelope. This creates different final states, depending on the **orientation of the spin** of the unpaired electrons



# Estimate of the signal intensity

Contribution of element A at depth d to photoemission signal

$$I_A = \Phi_X \times c_A(d) \times \sigma_{i,j}(h\nu) \times e^{-\frac{d}{\lambda \cos(\theta)}} \times A_{Analyzer} \times T_{Analyzer}$$

The diagram illustrates the contribution of each term in the equation to the signal intensity. Blue arrows point from each term to a corresponding label in a light green box:

- $\Phi_X$  points to Photon flux
- $c_A(d)$  points to Concentration of element A at depth d
- $\sigma_{i,j}(h\nu)$  points to Subshell ionization cross section
- $e^{-\frac{d}{\lambda \cos(\theta)}}$  points to Attenuation from depth d at detection angle  $\theta$
- $A_{Analyzer}$  points to Angular acceptance
- $T_{Analyzer}$  points to Analyzer transmission

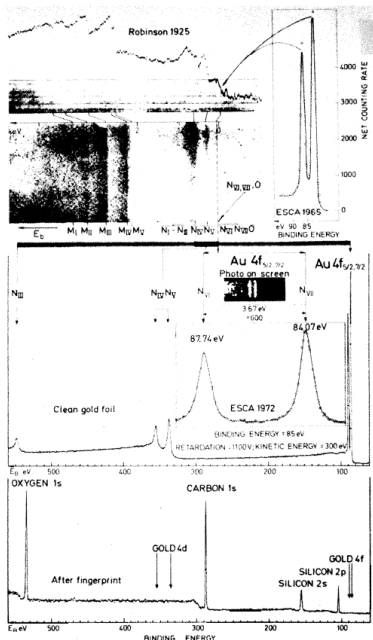
- Cross section -  $\sigma(\text{KE})$  - is the probability to have the photoemission event
- $10^{15}$  atoms  $\text{cm}^{-2}$  (equivalent to a monolayer) lead to about  $10^{-3}$  photoelectrons per incident photon
- Typical photon flux:  $10^{12} \text{ s}^{-1}$ , leads to about  $10^9$  photoelectrons  $\text{s}^{-1}$



# The development of XPS

1965

## First XPS Systems

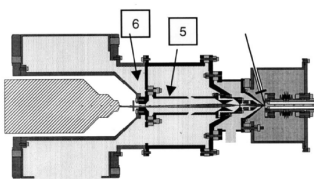
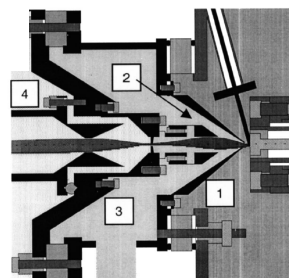
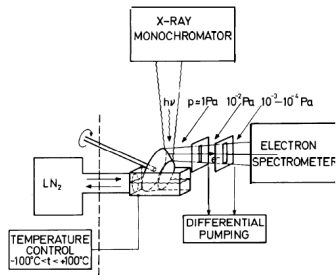


**UHV studies and first attempts to measure in the mbar (passive diff. pumping)**

K. Siegbahn, Nobel Lecture, 8 Dec 1981

2002

## First prototype of APXPS



## Differentially pumped electrostatic lens system

F. Ogletree et al. Rev. Sci. Instrum. 2002, 73, 3872

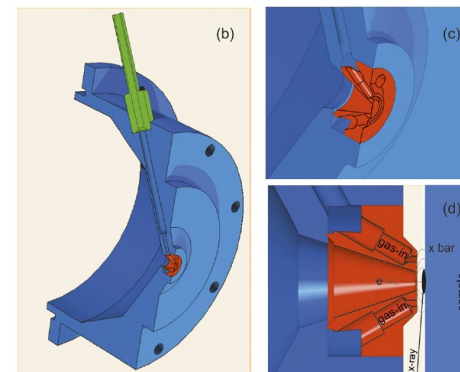
2005-



Commercial APXPS analyzers

2019

## Measurements at 1 bar and beyond



## Differentially pumped electrostatic lens system Tender x-rays + grazing angle detection

P. Amann et al. Rev. Sci. Instrum. 2019, 90, 103102

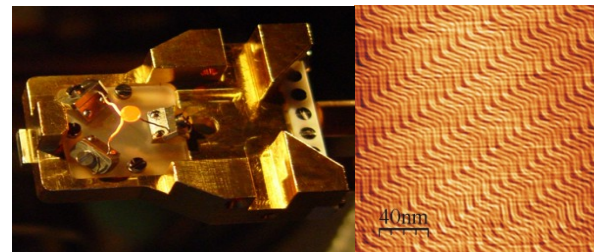
# Ambient pressure x-ray photoelectron spectroscopy

But...XPS is historically bound to high – ultra-high vacuum

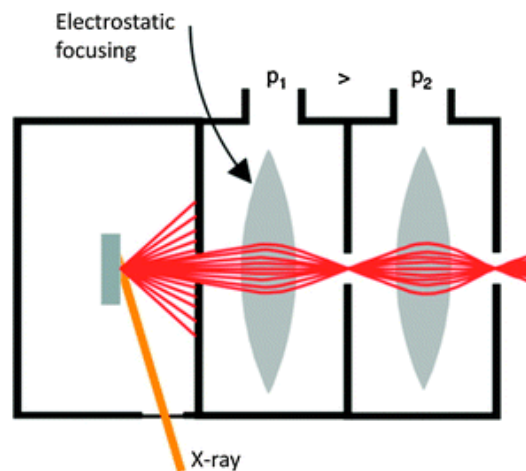
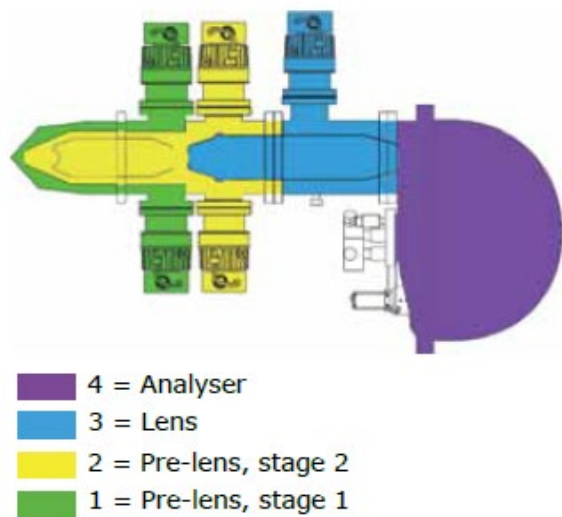
- **Pressure gap**



- **Material gap**



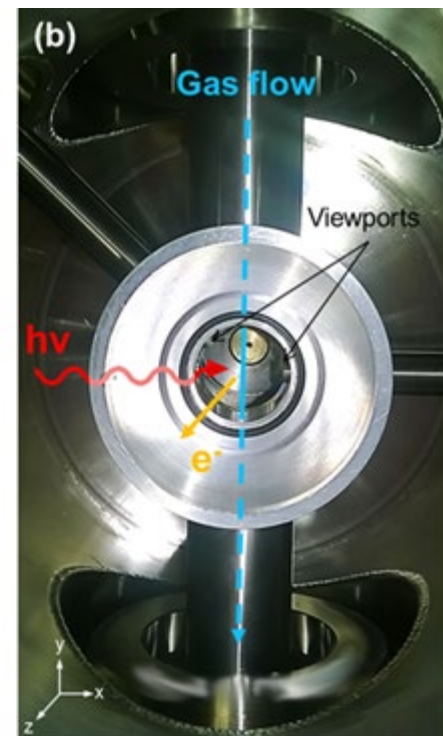
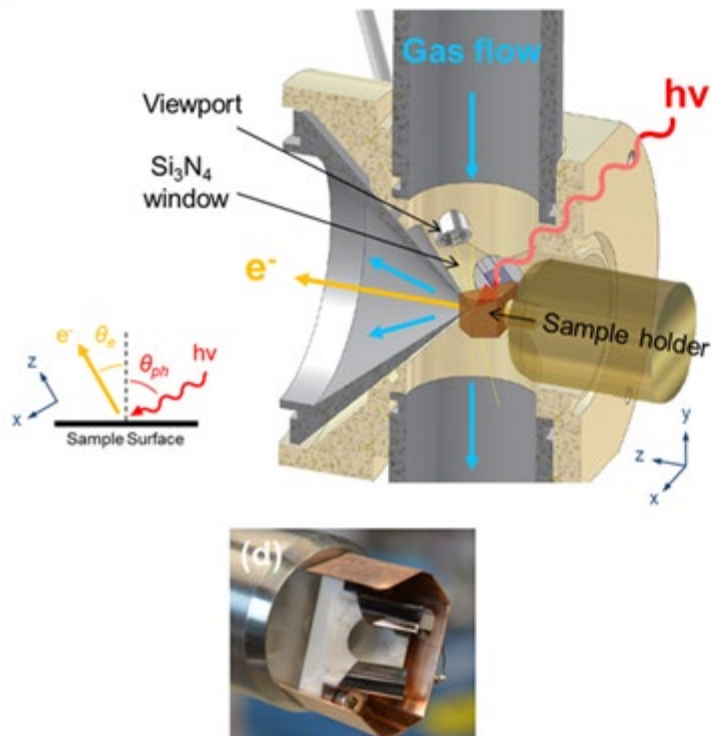
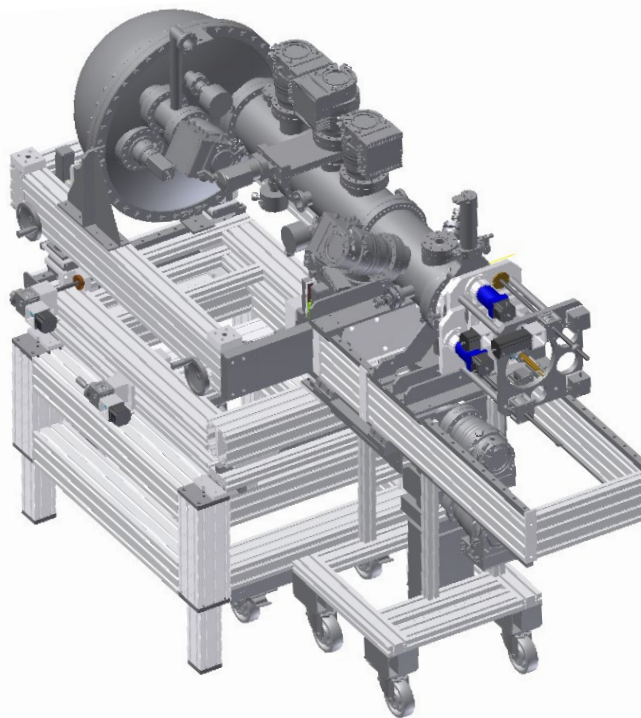
APXPS has partially filled the gaps!\*



- XPS up to 5 mbar (soft x-rays) and 50 mbar (tender x-rays)
- Possibility to investigate “real” samples (powders, semiconductors)

# Characterization of the solid-gas interface (SLS-PSI)

## Solid-gas interface endstation @X07DB\*

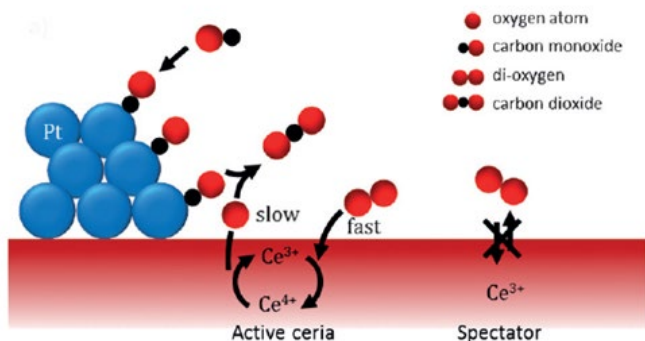


- Flow tube configuration
- Heated sample holder. Sample powder pressed, dispersed in ethanol and drop-casted on a gold foil

**Fast heating (e.g. from RT to stable 300°C in a few seconds)**

# 1) Carbon monoxide oxidation on Pt/CeO<sub>2</sub>

**Metal NPs (Pt, Pd, Au) supported on reducible oxides showed the best performance in the low temperature oxidation of carbon monoxide\***



- For **CeO<sub>2</sub>**: adsorption and activation of oxygen preferentially occur on the support, whereas carbon monoxide is adsorbed and supplied by the metal<sup>#</sup>

- Under catalytically relevant conditions: **rapid reoxidation of ceria**.
- Ce<sup>3+</sup> generated in the catalytic cycle is difficult too short lived to be detected **under steady state conditions**.

Studies employing **time-resolved techniques** are required to gather more information about the evolution of the active sites and their role in the reaction mechanism

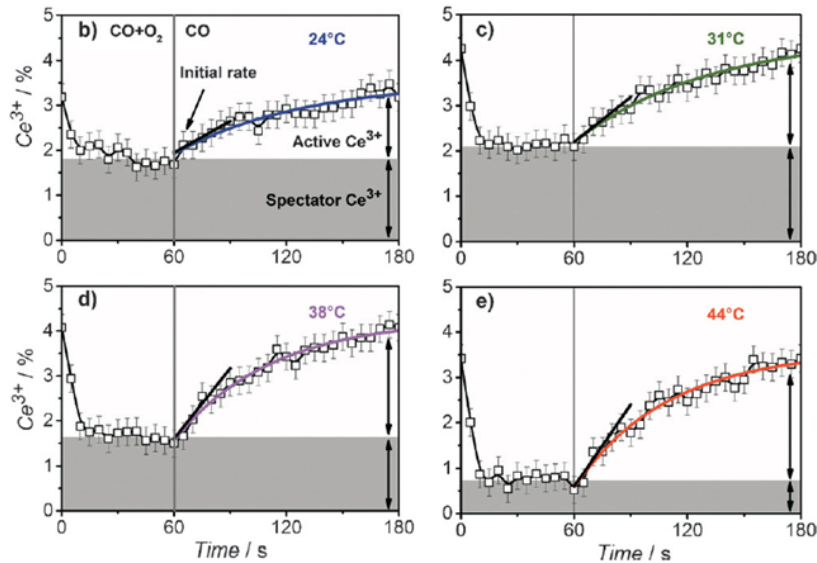
\* I. X. Green, et al., Science 2011, 333, 736. M. Carnello, et al., Science 2013, 341, 771. J. Saavedra, et al., Science 2014, 345, 1599.

<sup>#</sup> R. Kopelent, et al., Angew. Chem. Int. Ed. 2015, 54, 8728.

# Carbon monoxide oxidation on Pt/CeO<sub>2</sub>

Time-resolved RXES of Pt(1.5%)/CeO<sub>2</sub> (ca. 1.2 nm diameter Pt NPs on powdered ceria) – oxygen excess (1%CO, 4% O<sub>2</sub>)\*.

Pulsed experiment: from CO+O<sub>2</sub> to CO+inert



- The Ce<sup>3+</sup> concentration increases, thus oxygen from ceria participates in the oxidation of carbon monoxide.
- The initial rate of ceria oxidation is >10 times higher than that of reduction. Active Ce<sup>3+</sup> is **short lived**
- Presence of spectator Ce<sup>3+</sup> (not involved in the catalytic process) – probably formed during pretreatment of catalyst.

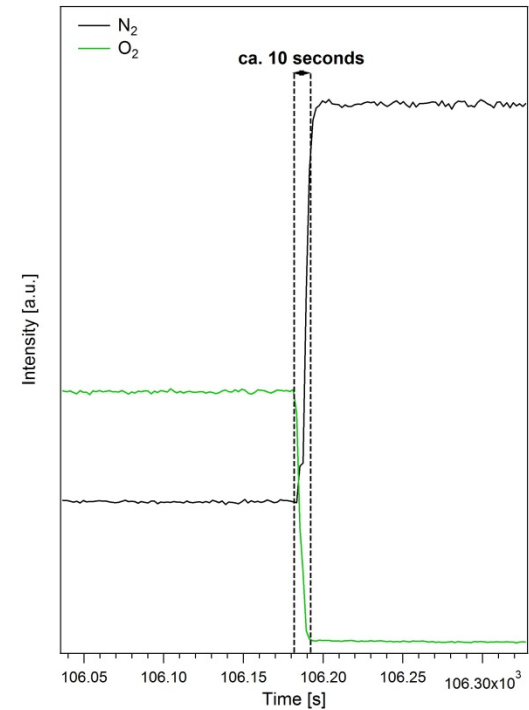
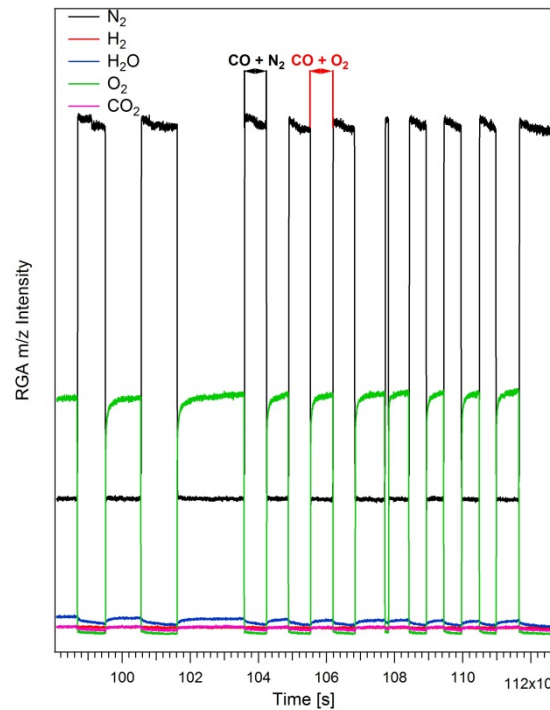
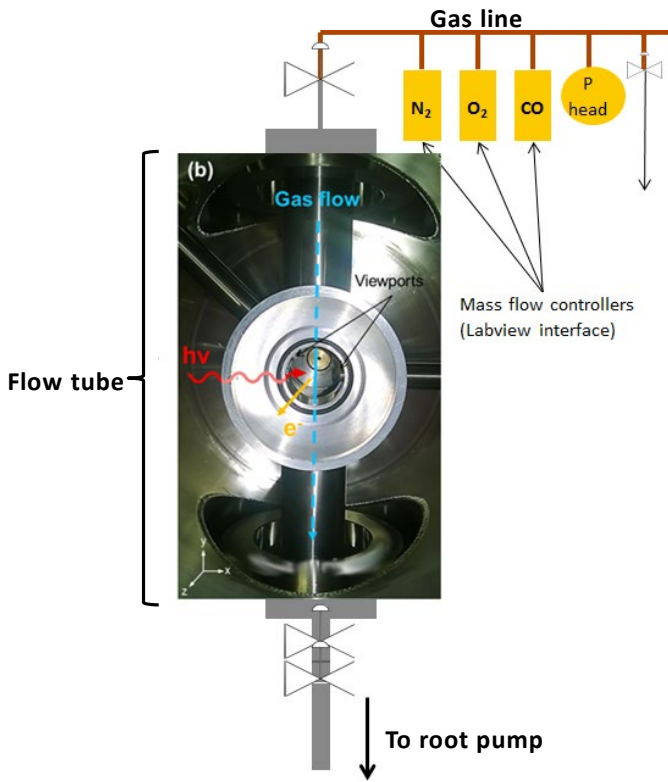
## OPEN ISSUES

- What is the effect of the activation in hydrogen?
- Are the active sites located at the metal/oxide interface? Exploit the surface sensitivity of XPS.



# Carbon monoxide oxidation on Pt/CeO<sub>2</sub>: experimental results

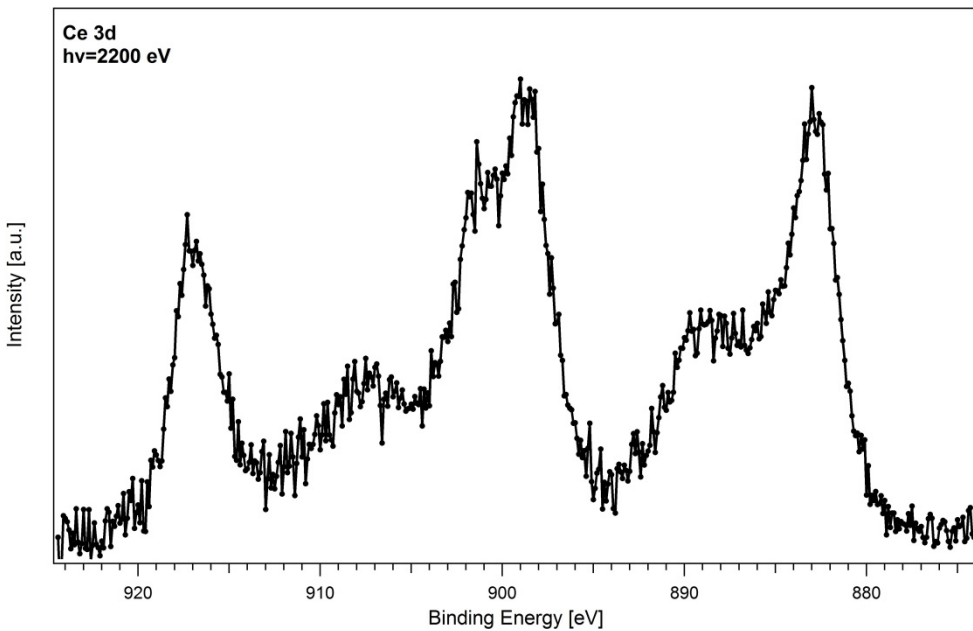
- Pressure in the flow tube stabilized (root pump) at **1.0 mbar**
- Switch on/off the oxygen while acquiring (CO:O<sub>2</sub> = 1:4)
- Oxygen replaced by nitrogen, same pressure and stable m/z signals in ca. 10-15 seconds



# Carbon monoxide oxidation on Pt/CeO<sub>2</sub>: experimental results

**Activation of the sample in hydrogen (150 °C, 1 hour, p=1.0 mbar)\***

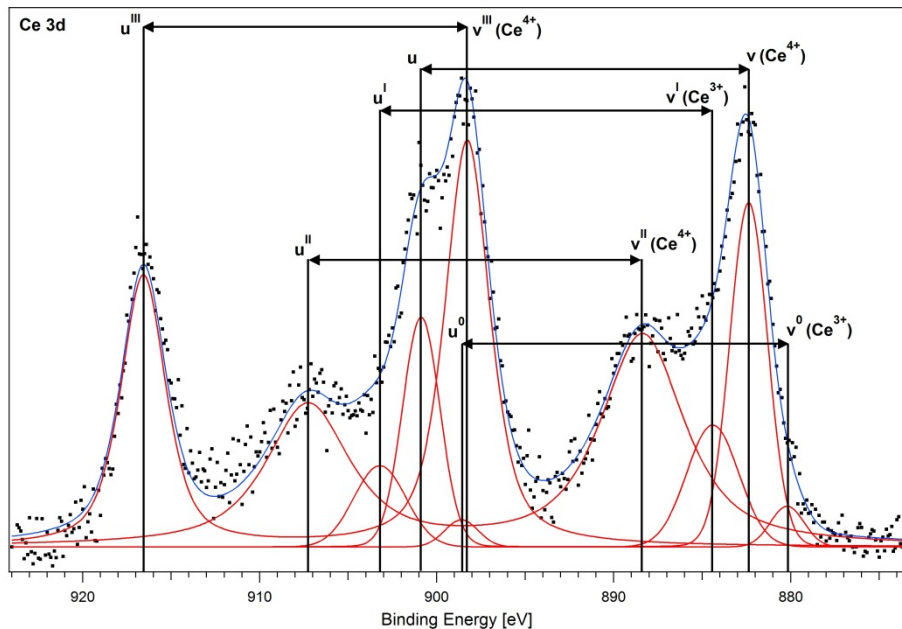
- Ce 3d acquired from 2.2 to 5.0 keV photon energy range



\*L. Artiglia, et al. J. Phys. Chem. Lett. 2017, 8, 102.

# Carbon monoxide oxidation on Pt/CeO<sub>2</sub>: experimental results

## Activation of the sample in hydrogen (150 °C, 1 hour, p=1.0 mbar)



- Ce 3d acquired from 2.2 to 5.0 keV photon energy range

The peaks can be separated into 5 *d* doublets<sup>#</sup>, associated to different final state configurations:

- $v^0$  and  $v^I$  are associated to **Ce<sup>3+</sup>**.
- $v$ ,  $v^{II}$  and  $v^{III}$  are associated to **Ce<sup>4+</sup>**.

\*L. Artiglia, et al. J. Phys. Chem. Lett. 2017, 8, 102.

<sup>#</sup>P. Burroughs, et al. J. Chem. Soc., Dalton Trans. 1976, 17, 1686-1698.



# Carbon monoxide oxidation on Pt/CeO<sub>2</sub>: experimental results

- Enhancement of the Ce<sup>3+</sup>/Ce<sup>4+</sup> ratio at low photon energy



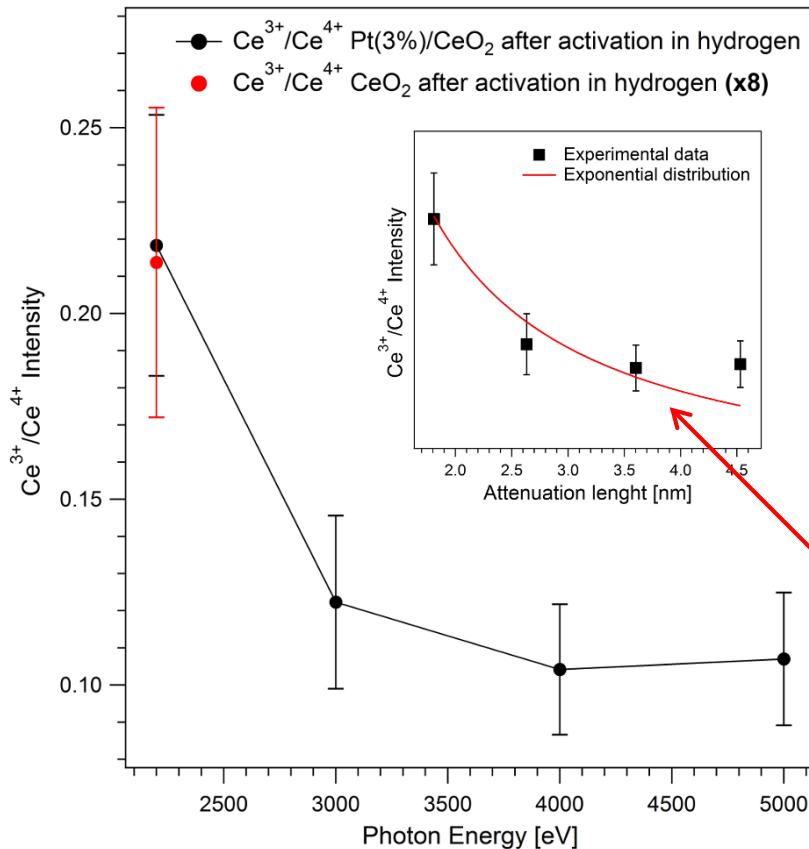
**Higher concentration of Ce<sup>3+</sup> sites is found at the surface\***

- On Pt free ceria (red dot) small amount of Ce<sup>3+</sup> detected only at 2.2.kev

Simple model (exp. distribution) used to fit the experimental data and quantify the depth of reduction of ceria on Pt/CeO<sub>2</sub>:#

$$\frac{I_o}{I_s} = \frac{F_o \rho_o \sigma_o \lambda_{o_o}}{F_s \rho_s \sigma_s \lambda_{s_s}} \cdot \frac{[1 - \exp(-t / \lambda_{o_o} \cos \theta)]}{\exp(-t / \lambda_{s_o} \cos \theta)}$$

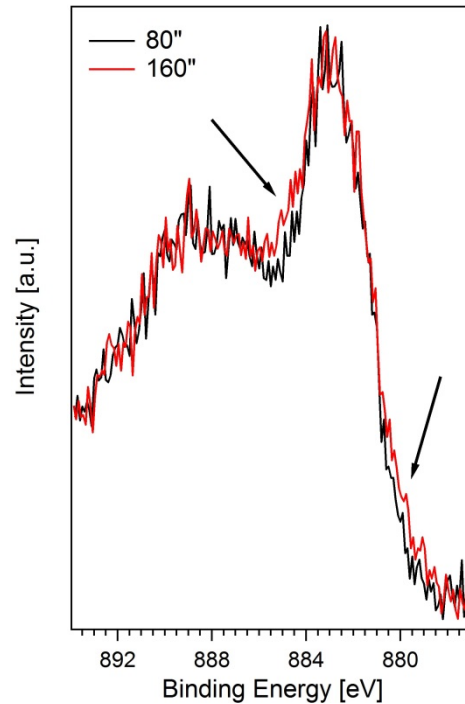
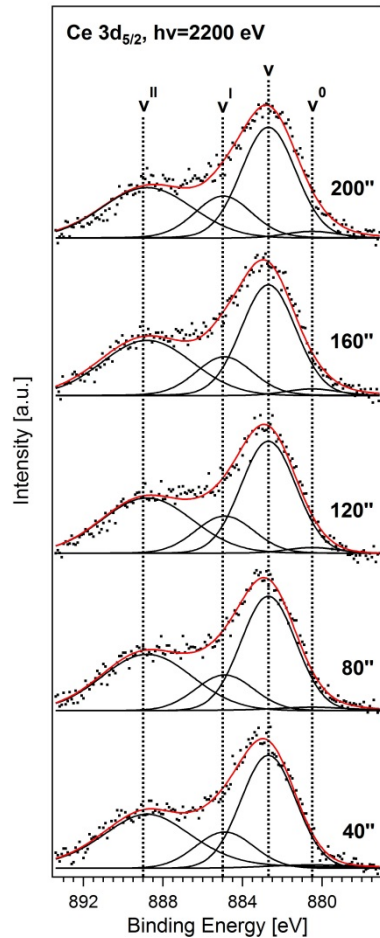
**t = 1.0 nm:** Ce<sup>3+</sup> sites are located in the outer layers of the ceria support, oxygen does not diffuse from the bulk to the surface.



\* S. Kato, Phys.Chem.Chem.Phys., 2015, 17, 5078.

# A. Cimino, et al. J. Electron Spectrosc. Relat. Phenom. 1999, 104, 1.

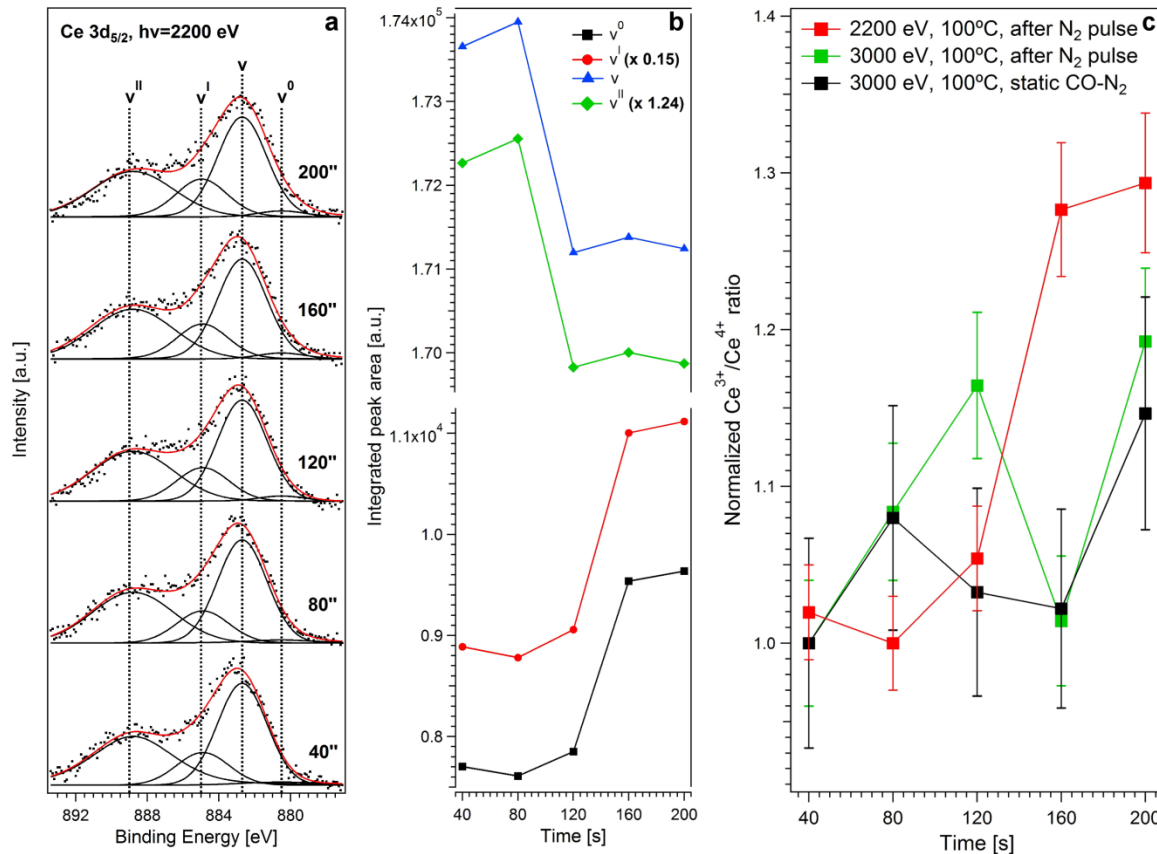
# Carbon monoxide oxidation on Pt/CeO<sub>2</sub>: experimental results



Fast scans (1 scan ~ 20") of the Ce 3d<sub>5/2</sub> at hv=2200 eV acquired immediately after switching from CO/O<sub>2</sub> to CO/N<sub>2</sub>

- The 3d<sub>5/2</sub> peak shape modifies between 80 and 160 seconds

# Carbon monoxide oxidation on Pt/CeO<sub>2</sub>: experimental results



- A constant background of Ce<sup>3+</sup> is visible throughout the experiment

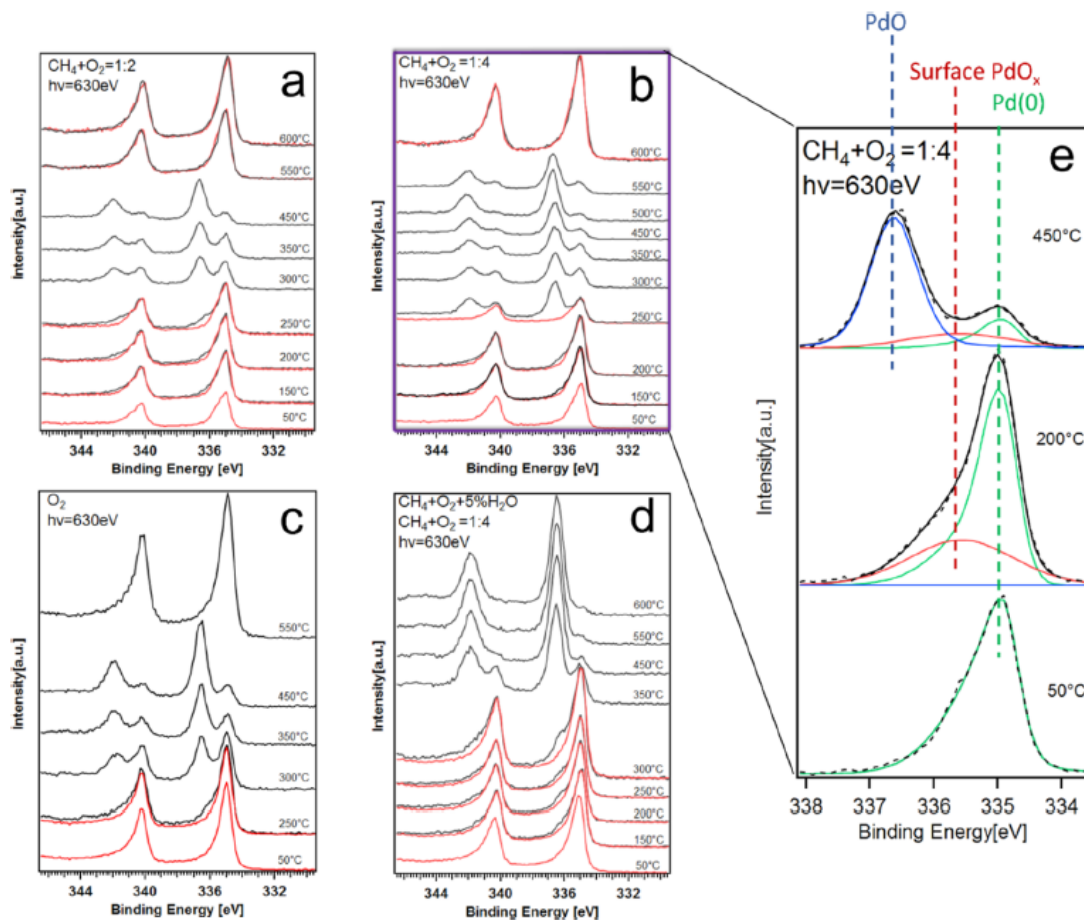


**Spectator sites:** formed after the activation, do not participate in the activation of oxygen

- The Ce<sup>3+</sup>/Ce<sup>4+</sup> ratio increases significantly between 80 and 160 seconds (2200 eV)
  - Same experiment at 3000 eV shows only **weak positive oscillations**
- ↓
- Catalytically involved Ce<sup>3+</sup> is at the surface**

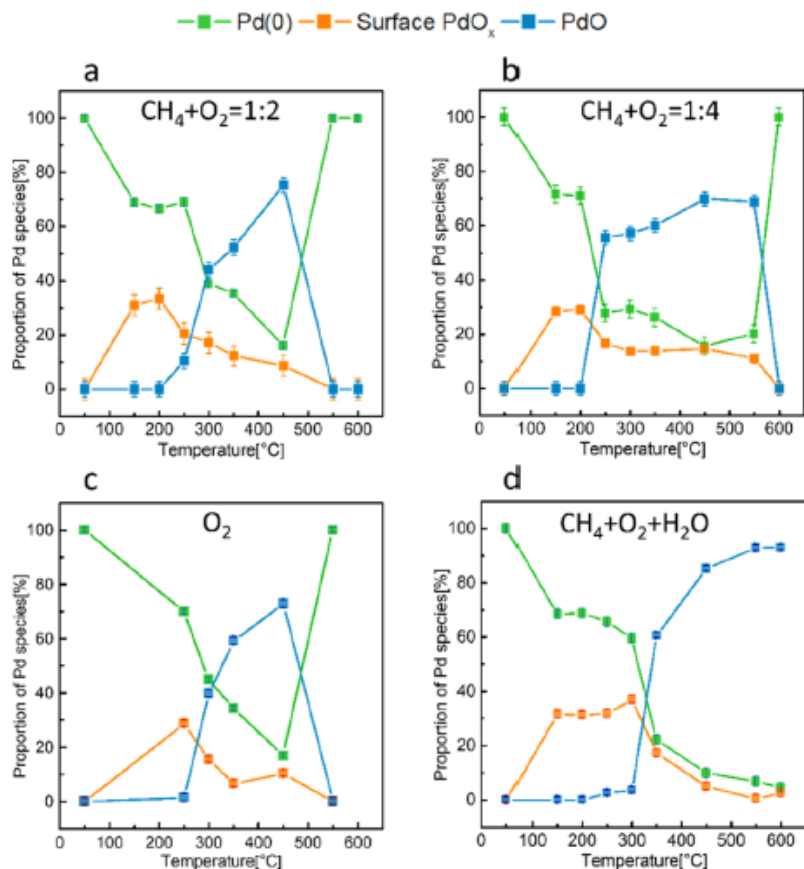
## 2) Methane oxidation on Pd foil (model surface)

- Pd foil, methane oxidation reaction → active sites and role of water
- Evolution of the Pd 3d signal exposed to different gas (reaction) mixtures in the methane oxidation reaction temperature range
- **It is known that water inhibits methane oxidation**



## 2) Methane oxidation on Pd foil (model surface)

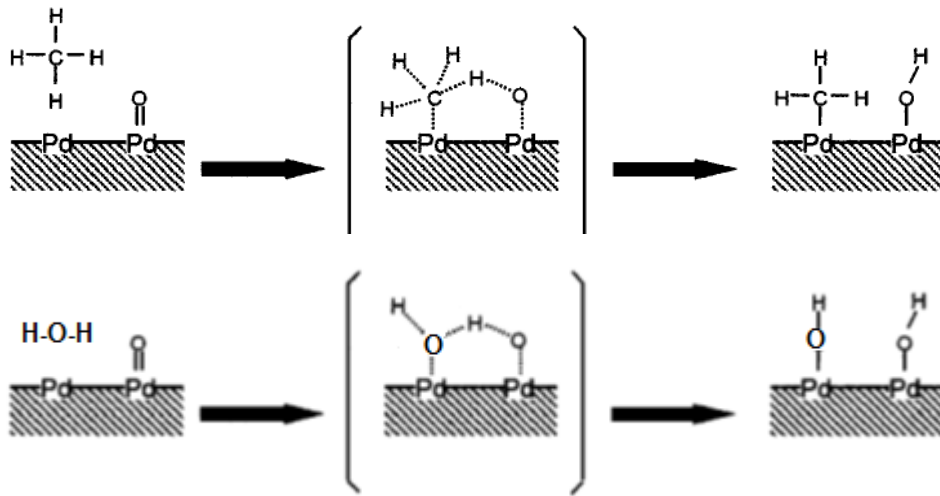
- Pd foil, methane oxidation reaction → active sites and role of water
- Evolution of the Pd 3d signal exposed to different gas (reaction) mixtures in the methane oxidation reaction temperature range



- Surface PdO<sub>x</sub> is a “precursor: under all conditions its growth onset is similar
- The onset of PdO growth depends on the reaction conditions:
  - 50°C delay in pure O<sub>2</sub> → could be due to the formation of stable surface oxide skin (no methane)
  - 100°C delay when H<sub>2</sub>O is co-fed → hindrance of O<sub>2</sub> activation/diffusion
- At 600°C palladium reduced back to metal, apart when water is dosed



Water delays the formation of the oxide (active phase). **WHY? Are surface –OH involved?**



Surface -OH form because of methane oxidation and water deprotonation

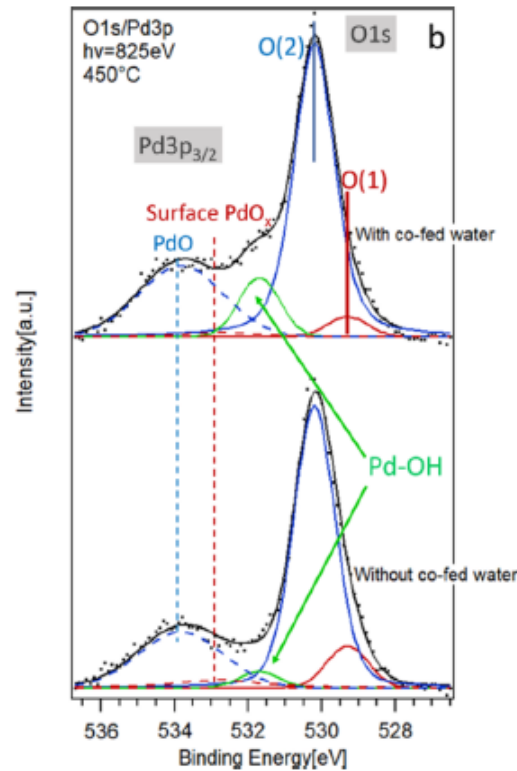
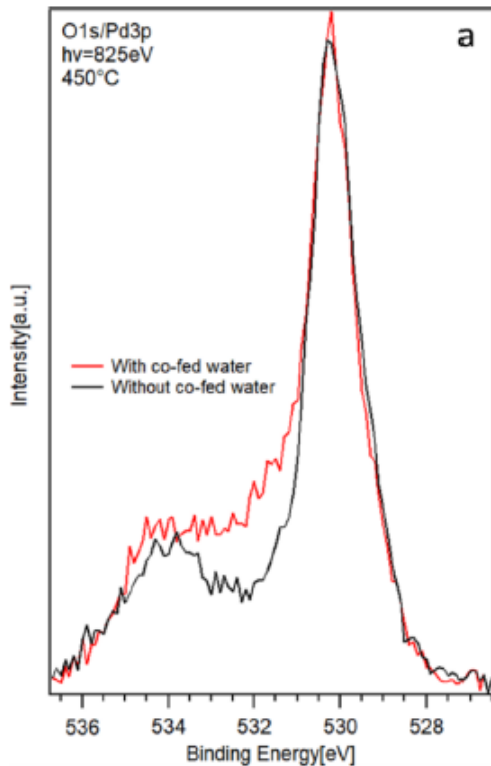


Signal of Pd-OH superimposed to that of PdO<sub>x</sub> in Pd 3d

We can explore the O 1s!



K.-i. Fujimoto, et al. J. Catal. 1998, 179, 431.



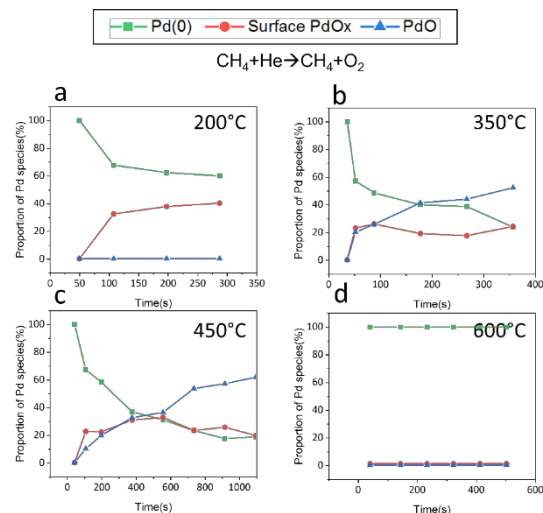
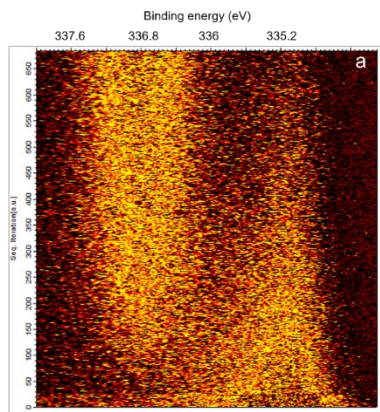
t=450°C – High % of PdO

- Also in the O 1s we see two oxide components (surface + bulk PdO<sub>x</sub>)
- When water is co-fed the peak of -OH increases by 3.5 times



Hydroxyls block the active sites for methane adsorption and activation

# Time-resolved analysis under transient conditions → particularly useful with **model systems\***

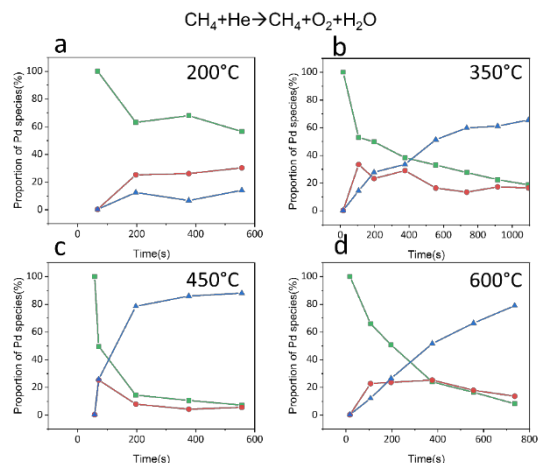
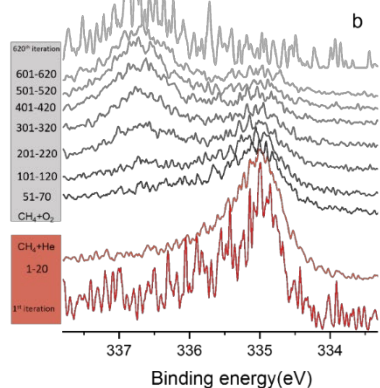


Initial formation rate of surface PdO<sub>x</sub> higher/equal to that of PdO



Surface PdO<sub>x</sub> is a precursor of PdO

The formation of PdO is delayed in the presence of water



- Water inhibits methane combustion converting surface PdO<sub>x</sub> to Pd-OH
- Formation of a relevant fraction of Pd-OH hinders the adsorption of gaseous O<sub>2</sub> and its diffusion to form PdO